Theoret. Chim. Acta (Berl.) 53, 21-54 (1979)

THEORETICA CHIMICA ACTA

An Intermediate Neglect of Differential Overlap Theory for Transition Metal Complexes: Fe, Co and Cu Chlorides

Allan D. Bacon

Guelph Waterloo Centre for Graduate Work in Chemistry, University of Guelph, Guelph, Ontario, Canada

Michael C. Zerner

Quantum Chemistry Group, University of Uppsala, Box 518, S-751 20 Uppsala, Sweden

and

Guelph Waterloo Centre for Graduate Work in Chemistry*, University of Guelph, Guelph, Ontario, Canada

A complete Intermediate Neglect of Differential Overlap model suitable for the examination of transition metal complexes is described. The model is characterized by the inclusion of all the one-center exchange terms necessary for rotational invariance and accurate spectroscopic predictions, as well as an accurate description of integrals involving 3*d* atomic orbitals. The model is within the unrestricted Hartree–Fock formalism, and a method for spin purification is described. Problems with convergence of the self-consistent field are discussed, and a method that has been found successful in aiding the convergence is outlined.

The model has been applied to many transition metal systems. In this article the results of calculations on the chlorides of Fe, Co and Cu are described. The results of these calculations are compared with experiment, and with the results of calculations by other methods.

Key words: INDO method for transition metals – Copper chloride – Iron chloride

1. Introduction

It is the purpose of this work to examine an approximate molecular orbital method capable of yielding useful information on the electronic structure of transition metal complexes, as well as yielding information and experience on the application of the molecular orbital approach itself, to such complexes. This report describes an Intermediate Neglect of Differential Overlap (INDO) model that is reasonably successful in describing the ground state properties of a large variety of transition

---

* Permanent address

0040-5744/79/0053/0021/$06.80

metal complexes. A subsequent paper will deal with the calculation of excited states.

Transition metal compounds are very often characterized by a high symmetry, suggesting that soundly developed and rationally parametrized molecular models should be as successful, if not more so, in describing the results of *ab initio* molecular orbital calculations as they are in describing molecules of hydrogen and the first row. Surely this high symmetry is behind the success of the crystal field and ligand field descriptions of such complexes [1]. The Iterative Extended Hückel theories have also been quite successful in yielding information on transition metal complexes [2, 3]; their success is due to a proper accounting for the molecular topology, and a high degree of parametrization on atomic data.

The Intermediate Neglect of Differential Overlap model is examined here [4]. This is one of the simplest theories that attempts to mimic in a more or less correct fashion the proper Born–Oppenheimer Hamiltonian. A simpler theory in the same spirit would be the Complete Neglect of Differential Overlap model (CNDO) [5], which differs from INDO by omitting the one-centre two-electron exchange terms. As we anticipate that differences between the energies of different spin states will be of interest, such a simplification will not be satisfactory. It is exactly these one-centre exchange terms that distinguish the various atomic term energies within an electronic configuration.

There are several rather unique problems met in studying the molecular orbital theory of transition metal complexes that are not met in dealing with molecules containing hydrogen and the first row atoms. The first of these is that the number of one-centre exchange integrals increases so greatly as to change the traditional zero-differential overlap method of formation of the Fock matrix in a direct fashion to methods in which the many integrals are calculated and ordered but once. A second difference is that metal *d* orbitals cannot be described accurately enough for most purposes by a single Slater type orbital and subsequent parameterization. Such an approach is "traditional" for other orbitals, or for *d* orbitals in second row atoms. Perhaps the most troublesome problem is that self-consistent field calculations on transition metal complexes seldom converge if the calculated molecular orbitals are used for the subsequent cycle, and if they do, often converge to an excited state.

Several other investigations have been made of Zero Differential Overlap (ZDO) models, and we will have recourse to discuss some of these methods later. This model will differ from all of them in the treatment of the one-centre metal exchange integrals, the structure of the *d* symmetry atomic orbitals, and, of course, the parameterization. Models that have proven useful and are not of the ZDO type are the Extended Hückel Methods of Zerner and Gouterman [2] and of Hoffmann [3], and the method of Hall and Fenske [6] which is based upon the Mulliken approximation for integrals.

After some rather extensive use of the INDO model, it is, perhaps, honest to note that the high symmetry and weak interactions that characterize transition metal compounds and that are the reasons for the success of simpler models, may well make methods that purport to more accuracy less useful unless refined. Models such as crystal field theory and the Extended Hückel theory might be said to lead to "physical orbitals" in which eigenvalues correspond more or less to ionization potentials or electron affinities, and orbital energy gaps correspond to spectral transitions, either directly, or perhaps, after simple correction [7]. Koopmans' approximation, however, which relates the negative of the orbital eigenvalue to an ionization potential, appears very unreliable in estimating ionization processes from either *ab initio* molecular orbital calculations or those obtained using the INDO model. Electrons removed from orbitals centred on metal atoms are often accompanied by 10–20 eV of relaxation energy, while those removed from ligand valence orbitals are accompanied by a relaxation of typically less than 1 eV. Because of this relaxation, the simple "intuitive" crystal field picture with metal *d* orbitals as the highest occupied, is often not obtained. Singly occupied metal *d* "MO's" are often buried below doubly occupied ligand MO's, even though the former are most easily ionized.

Worse than the loss of these simple "physical orbitals" is the realization that the role of configuration interaction (electron correlation) is very important when the interactions between atoms are weak. Typically a transition metal *is* weakly coupled to its ligands; very often a very simple Configuration Interaction (CI) completely changes the INDO description of the ground state. Without a great deal of care, self-consistent field molecular orbital calculations will converge to any one of several near lying states—not necessarily that of lowest energy, or to a state of cracked symmetry, again indicating an important role for CI. It may well prove that self-consistent field molecular orbital models, by themselves, will be of only limited utility in describing the electronic structure of transition metal complexes.

2. Description of the Method

We seek solutions of the molecular electronic Hamiltonian

$$H\psi = E\psi$$

where ψ is a function of all n valence electrons of the system. ψ will be approximated as a single Slater determinant

$$\psi = |\phi_1(1)\phi_2(2)\cdots\phi_n(b)|,$$

where $\{\phi_i\}$ are the molecular orbitals (MO's). For a closed shell system this will lead to the usual Restricted Hartree–Fock procedure (RHF) [8]; for an open shell system such a description will lead to the Unrestricted Hartree–Fock formalism (UHF) [9]. The methods developed would be equally as appropriate for RHF calculations on open shell systems [10], but this has, as yet, not been examined.

The molecular orbital ϕ_i is expanded as a linear combination of atomic orbitals as is conventional in the Roothaan–Hall recipe [8, 11]

$$\phi_i = \sum C_{i\alpha}\chi_\alpha \tag{1}$$

where $\{\chi_\alpha\}$ are the basis of atomic orbitals. Within the INDO approximation such orbitals are envisioned to be strongly orthogonal and are characterized in integrals by

$$\chi_\alpha^{\mathrm{A}}(1)\chi_\beta^{\mathrm{B}}(1)\,d\tau(1) = \chi_\alpha^{\mathrm{A}}(1)\chi_\beta^{\mathrm{A}}(1)\,d\tau(1)\delta_{\mathrm{AB}} \tag{2}$$

and

$$\begin{aligned}(\chi_\alpha^{\mathrm{A}}\chi_\beta^{\mathrm{A}} \mid \chi_\gamma^{\mathrm{B}}\chi_\delta^{\mathrm{B}}) &\equiv \int d\tau(1)\,d\tau(2)\chi_\alpha(1)\chi_\beta(1)r_{12}^{-1}\chi_\gamma(2)\chi_\delta(2)\\ &= \begin{cases}(\chi_\alpha^{\mathrm{A}}\chi_\beta^{\mathrm{A}} \mid \chi_\gamma^{\mathrm{A}}\chi_\delta^{\mathrm{A}}) & \mathrm{A} = \mathrm{B}\\ (\chi_\alpha^{\mathrm{A}}\chi_\alpha^{\mathrm{A}} \mid \chi_\gamma^{\mathrm{B}}\chi_\gamma^{\mathrm{B}})\delta_{\alpha\beta}\delta_{\gamma\delta} & \mathrm{A} \neq \mathrm{B}\end{cases}\end{aligned} \tag{3}$$

where χ_α^{A} "belongs" to atom A, χ_β^{B} to atom B. Equation (2) is the definition of the zero differential diatomic overlap approximation, Eq. (3) sets to zero two-centre two-electron terms involving one-centre differential overlap – the terms that distinguish the Neglect of Differential Diatomic Overlap model (NDDO) from INDO. It is hard to envision a basis set of atomic orbitals that has the property of Eq. (3); rather this approximation is usually justified by the relatively small size of $(\chi_\alpha^{\mathrm{A}}\chi_\beta^{\mathrm{B}} \mid \chi_\gamma^{\mathrm{B}}\chi_\delta^{\mathrm{B}})$ to $(\chi_\alpha^{\mathrm{A}}\chi_\alpha^{\mathrm{A}} \mid \chi_\gamma^{\mathrm{B}}\chi_\gamma^{\mathrm{B}})$, and the introduction of semi-empirical parameters that compensate for errors introduced by assuming Eq. (3).

Application of the variational principle yields the two matrix equations (4), (9).

$$\boldsymbol{F}^K\boldsymbol{C}^K = \boldsymbol{\Delta}\boldsymbol{C}^K\boldsymbol{\varepsilon}^K \tag{4}$$

$$\begin{aligned}F_{\mu\nu}^K &= T_{\mu\nu} - \sum_{\mathrm{B}} Z_{\mathrm{B}}(\chi_\mu|R_{\mathrm{B}}^{-1}|\chi_\nu) + \sum_{\sigma,\lambda}[P_{\sigma\lambda}(\chi_\mu\chi_\nu \mid \chi_\sigma\chi_\lambda) - P_{\sigma\lambda}^K(\chi_\mu\chi_\sigma \mid \chi_\nu\chi_\lambda)]\\ T_{\mu\nu} &\equiv (\chi_\mu|-\tfrac{1}{2}\nabla^2|\chi_\nu) + \nabla_{\mu\nu}\end{aligned} \tag{5}$$

where the superscript K refers to α or β electron spin. $\boldsymbol{F}$ is the Fock or energy matrix, $\Delta_{\mu\nu} = (\chi_\mu \mid \chi_\nu)$, the orbital overlap and $\boldsymbol{P} = \boldsymbol{P}^\alpha + \boldsymbol{P}^\beta$, the first order Fock–Dirac density matrix defined over the MO coefficients $\boldsymbol{C}^K$ as

$$P_{\mu\nu}^K = \sum_a^{\mathrm{MO}} N_a^K C_{a\mu}^K C_{a\nu}^K$$

with $N_a^K = 0$ or 1, the occupancy of ϕ_a^K.

Under the INDO model, Eqs. (5) become

$$\begin{aligned}F_{\mu\mu}^K &= U_{\mu\mu} - \sum_{\mathrm{B}\neq\mathrm{A}} Z_{\mathrm{B}}(\chi_\mu|R_{\mathrm{B}}^{-1}|\chi_\mu) + \sum_\sigma P_{\sigma\sigma}\gamma_{\mu\sigma} - P_{\mu\mu}^K\gamma_{\mu\mu} + \Delta G_{\mu\mu} \quad \mu \in \mathrm{A}\\ F_{\mu\nu}^K &= \beta_{\mu\nu} - P_{\mu\nu}^K\gamma_{\mu\nu} + \Delta G_{\mu\nu} \quad \mu \neq \nu\\ U_{\mu\mu} &\equiv (\chi_\mu|-\tfrac{1}{2}\nabla^2 - Z_{\mathrm{A}}/R_{\mathrm{A}}|\chi_\mu) + V_{\mu\mu}\\ \beta_{\mu\nu}^{\mathrm{AB}} &\equiv (\chi_\mu^{\mathrm{A}}|-\tfrac{1}{2}\nabla^2|\chi_\nu^{\mathrm{B}}) - \delta_{\mathrm{AB}}\sum_C Z_C(\chi_\mu^{\mathrm{A}}|R_C^{-1}|\chi_\nu^{\mathrm{B}})\\ \Delta G_{\mu\nu}^{\mathrm{AB}} &\equiv \left\{\sum_{\sigma,\lambda}^{\mathrm{A}}[P_{\sigma\lambda}(\mu\nu|\sigma\lambda) - P_{\sigma\lambda}^K(\mu\sigma|\nu\lambda)] + P_{\mu\nu}^K\gamma_{\mu\nu} - \sum_\sigma^{\mathrm{A}} P_{\sigma\sigma}\gamma_{\mu\sigma}\delta_{\mu\nu}\right\}\delta_{\mathrm{AB}}.\end{aligned} \tag{6}$$

In Eq. (6) $\gamma_{\mu\sigma} \equiv (\bar{\chi}_\mu\bar{\chi}_\mu \mid \bar{\chi}_\sigma\bar{\chi}_\sigma)$, where $\bar{\chi}_\mu$ is the s symmetry equivalent of χ_μ: for a one-centre integral $\gamma_{\mu\sigma} = F^0(\mu\sigma)$, the Slater–Condon integral [12]. The "A" above the summation indicates the sum is confined to only χ_σ on atom "A". With this definition, and $\Delta G_{\mu\nu} = 0$, the above are the Complete Neglect of Zero Differential (CNDO) Eqs. (5). For atoms with basis sets of s and p symmetry, the $\Delta G_{\mu\nu}$ are reasonably simple [4]. The inclusion of d symmetry orbitals, however, complicate these terms considerably. Rather than treat these terms in a general fashion in a double summation over integrals for each diagonal $F_{\mu\mu}$ for each cycle as is conventional for ZDO theories, it now becomes advantageous, as it does in *ab initio* calculations, to order and store the two electron integrals once. Each integral is then positioned in all places that it occurs in the two-electron G matrix as it is read. A summary of these INDO integrals appears in the Appendix. For an s and p basis these integrals are complete: for an s, p and d basis only those integrals corresponding to Slater–Condon G^K or F^K are kept.

Several investigators have suggested that "INDO" be interpreted as a theory that only keeps corrections corresponding to exchange $(\chi_\mu\chi_\nu \mid \chi_\mu\chi_\nu)$ and Coulomb $(\chi_\mu\chi_\mu \mid \chi_\nu\chi_\nu)$ type integrals. For an atom with an s, p basis, this is complete, but for atoms with d atomic orbitals the method is then rotationally variant. This variance is empirically small [13, 14], and can be removed by suitably averaging over classes of integrals [15].

We do not drop mixed integrals of the G^K or F^K type, for it is difficult to envision any basis set that avoids them. Although their omission in the SCF calculation does, indeed, seem small, we have found them to have a very important effect in the calculation of excited state transition energies, and in the calculation of correlation energy.

With these approximations, the formation of the Fock matrix is proportional to the number of integrals calculated, roughly n^2, where n is the size of the atomic orbital basis. Execution time of the SCF step is thus governed by the repeated solutions (diagonalizations) of Eq. (4).

3. Specification of Parameters

3.1. *Basis*

Equations (6) are general for a basis set of functions that display INDO. Insofar as the integrals of Eqs. (6) can be obtained empirically we need never specify the exact nature of the basis that yield Eqs. (2) and (3), and the value of the non-zero integrals. All integrals, however, cannot be found empirically for this work and as in the original CNDO and INDO model of Pople and co-workers [4, 5] we choose, for the present, a basis of Slater Type Orbitals (STO's), then envision them as symmetrically orthogonalized to one another, or midway along a bond "cut off" in such a fashion as to make Eq. (2) reasonable [16]. Since the values of two-electron matrix elements from such a basis does not seem to vary greatly from their value obtained with STO's (one-centre integrals are increased while two-centre are decreased, leaving the sums of Eq. (6) nearly constant [17]), the latter, much simpler evaluation is used. This is the conventional choice for the CNDO/2 and INDO/2 methods, but methods that are accurate in reproducing electronic spectra [18–20] and the popular MINDO methods [21, 22] choose these integrals and their functional form semi-empirically.

A basis set of single Slater-type orbitals (STO) is characterized by the choice of exponential constants. For hydrogen a value of 1.2 is taken. For elements of the first and second rows we use the exponents derived from Slater's rules [23], as do the original CNDO and INDO methods. More accurate values are available from the work of Clementi and Raimondi [24], but our results prove relatively insensitive to such minor changes.

For the elements of the third row, however, the exponents derived from Slater's rules are questionable. Also, single Slater orbitals are known not to be accurate representations of the *d* functions [25–28], as they concentrate too much electron density in the bonding region, causing an overestimation of the effective overlap, and the density beyond the bonding region falls off too rapidly with distance. Although linear combinations of STO's ("multiple-ζ" functions) are desirable for describing any atomic orbital, it appears that they are essential for describing the $3d$ orbitals. Nevertheless we would like to retain the simplicity of "single-ζ" functions, as adopting multiple-ζ representations greatly increases the length of the calculations, and is not in keeping with the spirit of the previous approximations.

In adopting this approach we realize that we cannot accurately represent the Hartree–Fock $3d$ functions everywhere, but we hope to be able to preserve the essential features, notably at $R = 0$ and in the bonding region. For $R = 0$, the functions are used in the evaluation of the F^0 integrals, and in the bonding region the functions are used to calculate the overlap integrals, which in turn are used to estimate the resonance integrals.

Using

$$\begin{aligned} F^0(d, d) &= 0.258138\,\zeta_{3d}(0) \\ F^0(s, s) &= 0.200905\,\zeta_{4s}(0) \end{aligned} \tag{7}$$

it is possible to calculate the best single exponents which will yield the F^0-values calculated from the Watson near-Hartree–Fock multiple-ζ functions [25]. In order to match the Watson near-Hartree–Fock $3d$ functions in both the bonding region and at $R = 0$ using single-ζ functions, we define ζ_{3d} as a function of the distance from the metal atom, R, and evaluate the exponent, $\zeta_{3d}(R)$, for the necessary R values. In doing this, we recognize that such a function may well not reproduce all the overlap interactions simultaneously, for in general, each of the $(s \mid d_\sigma)$, $(p_\sigma \mid d_\sigma)$ and $(p_\pi \mid d_\pi)$ overlap integrals will suggest a different ζ_{3d} value for any given R. The single ζ_{3d} that we would wish to use for all overlap integrals is a weighted average of the three exponents which reproduce the Watson overlaps [29, 30]. A procedure which weights each of the three exponents by the appropriate overlap could be used, but we choose to weigh the $(p_\pi \mid d_\pi)$ overlap by two, as it occurs twice in the calculation. From Table 1, it can be seen that the errors in the individual types of overlap are not large using single ζ_{3d} function for any given R.

Table 1. Nitrogen–metal overlap at various distances using the $3d$ values of Equation 8

Metal	Distance (in Å)	Overlap $(s \mid d_\sigma)$	Overlap $(p_\sigma \mid d_\sigma)$	Overlap $(p_\pi \mid d_\pi)$	Percentage error[a] s, d_σ	Percentage error[a] p_σ, d_σ	Percentage error[a] p_π, d_π
Ti	1.50	0.2361	0.2172	0.1908	10.9	−23.5	11.0
	2.054	0.1346	0.1541	0.0727	6.8	−11.8	8.1
	3.00	0.0285	0.0376	0.0097	4.1	−6.0	6.0
Fe	1.50	0.1487	0.1757	0.1178	9.9	−16.8	11.0
	2.054	0.0700	0.0958	0.0366	5.4	−9.7	7.7
	3.00	0.0102	0.0154	0.0034	3.3	−4.7	5.7
Zn	1.50	0.1024	0.1370	0.0797	6.4	−14.1	8.2
	2.054	0.0405	0.0606	0.0207	4.0	−7.2	6.6
	3.00	0.0045	0.0071	0.0014	2.2	−3.2	4.5

[a] $$\text{Error} = \left[\frac{\text{Overlap (Watson)} - \text{Overlap (Single)}}{\text{Overlap (Watson)}}\right]$$

Several functional forms for $\zeta_{3d}(R)$ have been examined to reproduce these single averaged exponents. Most successful is the simple form:

$$\begin{aligned} \zeta_{3d}(R) &= a + b/R \quad \text{for } \zeta_{3d}(R) < \zeta_{3d}(0) \\ \zeta_{3d}(R) &= \zeta_{3d}(0) \quad \text{elsewhere.} \end{aligned} \tag{8}$$

Although this form has the disadvantage of being discontinuous, it has the correct asymptotic behaviour and the greatest accuracy at 1.5 Å, 2.054 Å and 3.0 Å of the simple forms we have tried. Table 2 gives the values of the variables a and b, as well as the calculated exponential values.

The use of Eq. (8), perhaps, requires some further comment. It is chosen for simplicity, and merely as a trick to allow a single-ζ representation of a multiple-ζ function. That is, we envision that we are using the multiple-ζ functions given by Watson, but are approximating the integrals by the use of Eq. (8). No further interpretation makes sense.

Since a single value for ζ_{4s} appears to be reasonably accurate at $R = 0$ and at $R = 2.054$ Å, we adopt Zerner's "best single" values [29]. We set the $4p$ exponent equal to that of the $4s$, in analogy with the first and second row elements. Alternate exponents are available from the work of Richardson, Powell and Nieuwpoort [26] but these $4p$ functions prove too diffuse, leading in many cases to negative orbital electronic populations [29]. Labarre and co-workers [31, 32] adopt $4p$ exponents even smaller than those of Nieuwpoort in their CNDO/2 method for transition metals in order to reduce the $4p$ electronic populations. They have chosen, however, to compare their density over orthogonalized orbitals with the results of a population analysis from *ab initio* results, a procedure the validity of which is suspect. We believe their $4p$ orbitals are too diffuse.

Clack and co-workers [13] adopt the Zerner set of $3d$ and $4s = 4p$ exponents, after extensive comparative studies using Slater, Clementi's best single [24], and Burns' [33] exponents. This introduces an error in the evaluation of the one-centre $3d$

Table 2. Constants for the functional form $a + b/R$ of $\zeta_{3d}(R)$ and some resulting values

Atom	a	b	R				
			1.50	2.054[f]	3.00	4.00	∞
Ca[c]	1.5097	0.8105					
Sc[c]	1.6102	0.8961					
Ti	1.71016	0.96428	[d] 2.3530	2.1796	2.0316	1.9512	1.7102
			[e] 2.3799	2.1678	1.9951	1.9081	1.7316
V	1.81119	1.04854	[d] 2.5102	2.3217	2.1607	2.0733	1.8112
			[e] 2.5316	2.3137	2.1296		1.8289
Cr	1.91367	1.10712	[d] 2.6518	2.4527	2.2827	2.1905	1.9137
			[e] 2.6651	2.4509	2.2586		1.9262
Mn	2.0152	1.17510	[d] 2.7986	2.5873	2.4069	2.3090	2.0152
			[e] 2.8061	2.5890	2.3892		2.0235
Fe	2.11093	1.22250	[d] 2.9259	2.7061	2.5184	2.4166	2.1109
			[e] 2.9382	2.7009	2.5015	2.3948	2.1208
Co	2.21589	1.23008	[d] 3.0359	2.8148	2.6259	2.5234	2.2159
			[e] 3.0362	2.8190	2.6192		2.2181
Ni	2.31682	1.26242	[d] 3.1584	2.9314	2.7376	2.6324	2.3168
			[e] 3.1544	2.9371	2.7374		2.3154
Cu	2.41805	1.29449	[d] 3.2810	3.0483	2.8495	2.7417	2.4181
			[e] 3.2725	3.0552	2.8565		2.4127
Zn	2.51974	1.33244	[d] 3.4080	3.1684	2.9639	2.8529	2.5197
			[e] 3.3944	3.1769	2.9788	2.8716	2.5100

[c] From quadratic extrapolation.
[d] Calculated from $\zeta_{3d}(R) = a + b/R$.
[e] ζ_{3d} averaged to match Watson overlap (see text).
[f] Note that the $\zeta_{3d}(2.054)$ values are virtually the same as the Zerner "best single" exponents, Ref. [29].

integrals, $F^0(dd)$. Although part of this discrepancy will be removed by cancellation between the one-electron and two-electron energy matrices, it will be sizeable for transition elements with a large net charge.

In concluding this section, our choice of transition metal exponents give a nearly "exact" result for the only one-centred integral evaluated, F^0 [25]. At bonding distances, the only integral evaluated will be the overlap integral and the two-centred Coulomb integrals. Here we will weight this overlap by empirical factors in forming the resonance integrals, reducing the effect of any errors. At large internuclear separation (where the overlap, and thus errors, are small anyway), the most diffuse of the multiple-ζ functions will dominate, and the parameter "a" of Eq. (8) is chosen to yield this correctly. F^0 is the accurate Watson value by our use of Eq. (7). The two-centred Coulomb integrals at bonding distances seem accurately represented, and at further distances are essentially $1/R$.

3.2. One-Centre Core Integrals

The one-centre core integrals $U_{\mu\mu}$ are defined in Eq. (6). While these integrals could be calculated over an orthogonalized basis and corrected by a core pseudo-potential $V_{\mu\mu}$ that simulates the repulsion of the inner shell electrons [34], conventional CNDO and INDO methods relate these integrals to parameters obtained from atomic ionization potentials or from ionization potentials and electron affinities [4, 5]. They might also be obtained from atomic spectral terms [35], or from the orbital energies of atomic calculations [6].

We choose to calculate core integrals from ionization processes, with the hope that such a choice will aid in the interpretation of our molecular orbital eigenvalues.

An analysis of the average energy of an atomic configuration yields [12, 35]

$$\begin{aligned} I_s &= E(s^{l-1}p^m d^n) - E(s^l p^m d^n) \\ &= -U_{ss} - (l-1)F^0(s,s) - m[F^0(s,p) - \tfrac{1}{6}G^1(s,p)] \\ &\quad - n[F^0(s,d) - \tfrac{1}{10}G^2(s,d)] \\ I_p &= E(s^l p^{m-1} d^n) - E(s^l p^m d^n) \\ &= -U_{pp} - (m-1)[F^0(p,p) - \tfrac{2}{25}F^2(p,p)] \\ &\quad - l[F^0(s,p) - \tfrac{1}{6}G^1(s,p)] - n[F^0(p,d) - \tfrac{1}{15}G^1(p,d) - \tfrac{3}{70}G^3(p,d)] \\ I_d &= E(s^l p^m d^{n-1}) - E(s^l p^m d^n) \\ &= -U_{dd} - (n-1)[F^0(d,d) - \tfrac{2}{63}(F^2(d,d) + F^4(d,d))] \\ &\quad - l[F^0(s,d) - \tfrac{1}{10}G^2(s,d) \\ &\quad - m[F^0(p,d) - \tfrac{1}{15}G^1(p,d) - \tfrac{3}{70}G^3(p,d)]. \end{aligned} \tag{13}$$

The F integrals are calculated exactly for the basis, assuming the effective single exponential constant given in the previous section. The other Slater–Condon factors that occur in the theory are taken as semi-empirical parameters: they are presented in Table 3.

The valence state ionization potentials I_i are estimated from atomic spectroscopy [39]. The complete set of numerical values for the atoms up to and including Zn is given in Table 4. In this table, two sets of ionization potentials are given for the transition metals Ca–Cu, since both $d^{n-1}s$ and $d^{n-2}s^2$ are possible lowest average energy configurations of these atoms. For most atoms, the choice of the electron configuration is obvious, but for the transition metals it is not.

We therefore define two sets of processes dependent on the configuration of the transition metal atom:

$$\begin{array}{lll} \text{Process 1:} & I_s & 3d^{n-1}4s \rightarrow 3d^{n-1} \\ & I_p & 3d^{n-1}4p \rightarrow 3d^{n-1} \\ & I_d & 3d^{n-1}4s \rightarrow 3d^{n-2}4s \\ \text{Process 2:} & I_s & 3d^{n-2}4s^2 \rightarrow 3d^{n-2}4s \\ & I_p & 3d^{n-2}4s4p \rightarrow 3d^{n-2}4s \\ & I_d & 3d^{n-2}4s^2 \rightarrow 3d^{n-3}4s^2 \end{array}$$

These ionization processes yield the two sets of values given in Table 4. Clack and co-workers [13] use Process 2 for all the transition metals in their CNDO and INDO methods, but an examination of the average observed configuration promotion energies, clearly shows that the $d^{n-2}s^2$ configuration is not the lowest configuration in every case [29], and that this choice effects calculated ground state

Table 3. Slater–Condon factors (in cm^{-1})

At. no.	Atom	$G^1(s, p)$[a]	$F^2(p, p)$[a]	$G^2(s, d)$[d]	$G^1(p, d)$[d]	$F^2(p, d)$[d]	$G^3(p, d)$[d]	$F^2(d, d)$	$F^4(d, d)$[d]
3	Li	20194[b]	10944[b]						
4	Be	30876	21425						
5	B	43566	28075						
6	C	55635	36375						
7	N	72255	52100						
8	O	95298	55675						
9	F	116828[b]	69310[b]						
10	Ne	—	—						
11	Na	13450[c]	6000[c]	3042	9224	11000	5506	7477	4876
12	Mg	19974	26400	3885	3070	4416	1833	7477	4876
13	Al	27093	12925	1426	1896	3461	1130	7477	4876
14	Si	38814	18250	14496	2506	19675	11828	19438	12677
15	P	8541	23775	19081	25334	23176	15124	23925	15603
16	S	24807	36600	25972	34486	29173	20587	28411	18529
17	Cl	71000[c]	52000[c]	17131	2274	5102	1358	12860	8387
18	Ar	—	—						
19	K	8986[c]	4000[c]						
20	Ca	12600	2325	3730	5890	4480	−238	18900	9500
21	Sc	12100	5000	5870	5650	11000	2210	29500	14600
22	Ti	13100	5500	6200	7320	13700	10300	44900	29700
23	V	15100	6000	6240	5180	11200	1710	50800	35400
24	Cr	14400	6500	5220	5580	11400	297	63500	36800
25	Mn	18900	7000	6110	1240	8010	4970	66000	37900
26	Fe	16300	7500	6640	2450	5020	3520	61000	38400
27	Co	22700	8000	6340	3170	6290	2260	64500	48100
28	Ni	19400	8500	6700	3010	6050	3250	79800	53300
29	Cu	20700	9000	4460	5620	10700	6930	85980	57965
30	Zn	20400	9500						

[a] $G^1(2s, 2p)$, $G^1(3s, 3p)$, $F^2(2p, 2p)$ and $F^2(3p, 3p)$ from Ref. [40] unless otherwise designated. $G^1(4s, 4p)$ and $F^2(4p, 4p)$ from Ref. [41].

[b] From Ref. [4].

[c] Ref. [42].

[d] Na–Cl are calculated from atomic spectra and isoelectric extrapolation; Ca–Cu are values calculated by Anno and Teruya, Ref. [41].

Table 4. Ionization potentials (eV) for Eq. (13)

Atom	$-I_s$	$-I_p$	$-I_d$
H	13.06[a]		
He	—	—	
Li	5.39	3.54	
Be	9.32	5.96	
B	14.05	8.30	
C	19.84	10.93	
N	25.69	14.05	
O	32.90	17.28	
F	39.39	20.86	
Na	5.14	3.04	1.52
Mg	7.64	4.52	1.74
Al	11.33	5.98	1.96
Si	15.13	7.67	2.05
P	18.66	10.78	3.50
S	21.11	12.39	4.11
Cl	25.23	15.03	6.
K	4.34	2.73	1.67

	$d^{n-2}s^2$ [b,c]			$d^{n-1}s$ [b,c]		
	$-I_s$	$-I_p$	$-I_d$	$-I_s$	$-I_p$	$-I_d$
Ca	6.03	3.96	—	5.13	2.99	3.44
Sc	6.72	4.20	8.16	5.83	3.43	4.85
Ti	7.28	4.48	9.07	6.34	3.75	5.93
V	7.73	4.77	9.89	6.71	3.95	6.77
Cr	8.07	5.04	10.66	6.97	4.06	7.43
Mn	8.35	5.27	11.45	7.15	4.10	7.99
Fe	8.76	5.42	12.31	7.27	4.08	8.53
Co	9.94	5.48	13.30	7.38	4.02	9.10
Ni	9.13	5.41	14.46	7.51	3.93	9.79
Cu	9.36	5.18	15.87	7.69	3.84	10.67
Zn	3.54	4.77	17.57	—	—	—

[a] For H this corresponds to the ionization potential for an orbital exponent of 1.2.

[b] For the associated ionization processes refer to text.

[c] From Ref. [29].

properties. With very little ambiguity we choose as lowest the $d^{n-1}s$ configuration for Ni and Cu, and the $d^{n-2}s^2$ configuration for Ca, Sc, Ti and Zn. It is also likely that the $d^{n-1}s$ configuration is appropriate for Fe and Co, and the $d^{n-2}s^2$ configuration for V. For Cr and Mn it is not possible to decide the configuration because there are simply too few states known. The choice of configuration for these two atoms then were made *a posteriori*, that is, from the results of actual calculations. The calculation of ground state geometries seems definitive in this regard, with both atoms then being assigned the $d^{n-2}s^2$ average configuration as yielding the best results.

3.3. The Resonance Integral

The "resonance" integral, or "bonding parameter" $\beta_{\mu\nu}$ is given in Eq. (6). Its exact evaluation over orthogonalized orbitals is often difficult and requires an exact specification of the basis [36]. In addition, the value of $\beta_{\mu\nu}$ and its distance dependence is very sensitive to the details of the basis set orthogonalization. There exists, as yet, no complete theoretical formulation of the resonance integral, although several attempts have been made in this direction. At present, the formulation of the resonance integral is the weakest aspect of any zero differential overlap theory.

We shall set one-centre resonance integrals to zero. This seems strongly suggested by the work of Seamans and Linderberg [37] and Zerner and Parr [16], and is conventional in INDO methods.

For the two-centre one-electron integral we use [5, 38]

$$\beta_{\mu\nu} = (\beta^{\mathrm{A}} + \beta^{\mathrm{B}})\bar{S}_{\mu\nu}/2$$

with

$$\begin{aligned} \bar{S}_{ss'} &= \Delta_{ss'} \\ \bar{S}_{sp'} &= \Delta_{sp'} \\ \bar{S}_{pp'} &= g_\pi f_{p\pi}\Delta_{p\pi p\pi} + g_\sigma f_{p\sigma}\Delta_{p\sigma p\sigma} \\ \bar{S}_{sd'} &= \Delta_{sd} \\ \bar{S}_{pd} &= g_\pi f_{d\pi}\Delta_{p\pi d\pi} + g_\sigma f_{d\sigma}\Delta_{p\sigma d\sigma} \\ S_{dd} &= g f'_{d\delta}\Delta_{d\delta d\delta} + g_\pi f'_{d\pi}\Delta_{p\pi d\pi} + g_0 f'_{d\sigma}\Delta_{p\sigma d\sigma} \end{aligned} \tag{16}$$

where $\bar{S}_{\mu\nu}$ is a weighted orbital overlap, g_μ are the geometric factors necessary to convert from the local diatomic coordinate system to the molecular system, and f_μ and f'_μ are universal weighting factors for sigma, pi and delta types of interactions.

Considering an atom of s, p type basis, Eq. (16) relates the five possible diatomic interactions, ss', sp'_σ, $p'_\sigma s$, $p_\sigma p'_\sigma$, and $p_\pi p'_\pi$ to the single parameter β^{A} through the orbital overlap, and thus the basis actually used. Through the introduction of $f_{p\pi}$ and $f_{p\sigma}$ we loosen this specificity, but, of course, at the introduction of two parameters. As $f_{p\pi}$ and $f_{p\sigma}$ will not be chosen to be distance dependent, "non-nearest neighbour" $\beta_{\mu\nu}$ will be related to nearest neighbour through the distance dependence of the STO overlap. This is a serious disadvantage but probably succeeds as the necessary symmetry requirements of $\beta_{\mu\nu}$ are met by the overlap, and non-nearest neighbour $\beta_{\mu\nu}$'s are calculated small. Del Bene and Jaffé [19] have set $f_{p\pi} = 0.585$ to obtain results from CNDO in good accord with molecular electronic spectra. Ridley and Zerner [18] introduced the addition factor $f_{p\sigma} = 1.267$ that gave improved results for n–π^* excitations. In addition Ridley and Zerner found that $f_{p\pi} = 0.68$ gave an improved triplet spectrum [20]. Without an extensive parameter search, we have set $f_{p\pi} = 0.64$, an average value, and $f_{p\sigma} = 1.267$. The MO eigenvalue spectra obtained with such a choice, and especially the positioning of pi symmetry MO's with respect to those of sigma symmetry, compare well with model *ab initio* calculations for the systems we have examined.

When Eq. (11) is extended for use with *d* symmetry AO's it is no longer possible to use a unique β_{A} for each atom. Two such parameters are used, one for *s* and *p*, and the other for *d*. Labarre *et al.* [31, 32], on the basis of population studies on transition metal complexes have suggested that, for transition metals,

$$\beta_{4s}^{\mathrm{A}} \neq \beta_{4p}^{\mathrm{A}}$$

Our choice of $\beta_{4s,p}^{\mathrm{A}} \neq \beta_{3d}^{\mathrm{A}}$ introduces a variance to hybridization between the two shells, but we find this a small price to pay for the greatly improved results. We set $f_{d\pi} = f_{d\sigma} = 1$, and empirically search only the value of β_{3d}^{A}. We have not, as yet, examined in detail complexes of two transition metals, and defer comment on $f'_{d\delta}$, $f'_{d\pi}$ and $f'_{d\sigma}$.

The $\beta_{\mathrm{A}(D)}^{Q}$ values selected are given in Table 5.

3.4. Nuclear Electronics Attraction

According to Eq. (6) the nuclear attraction integral $(\chi_\mu | R_C^{-1} | \chi_\nu)$ appear in $\beta_{\mu\nu}^{\mathrm{AB}}$ and $F_{\mu\mu}$. For A = B $\beta_{\mu\nu}^{\mathrm{AA}} = 0$, for reasons given in the previous section. For A ≠ B the integral $(\chi_\mu^{\mathrm{A}} | R_C^{-1} | \chi_\nu^{\mathrm{B}})$ vanishes under the INDO approximation, Eq. (2). The integrals $(\chi_\mu^{\mathrm{A}} | R_C^{-1} | \chi_\mu^{\mathrm{A}})$ that occur in $F_{\mu\mu}$ are set equal to γ_{AC}

$$\gamma_{\mathrm{AC}} = (\chi_\mu^{\mathrm{A}} | R_C^{-1} | \chi_\mu^{\mathrm{A}}) \tag{17}$$

Table 5. The bonding parameter β_A^0(eV)[a]

Atom	$-\beta(s)$	$-\beta(d)$
H	9.0	
Li	9.0	
Be	13.0	
B	17.0	
C	22.4	
N	27.6	
O	34.2	
F	39.0	
Na	7.72	
Mg	9.45	
Al	11.3	
Si	(13.0)	
P	(15.1)	
S	16.0	
Cl	18.0	
Ca	−2.0	11.4
Sc	1.0	15.0
Ti	1.0	18.0
V	1.0	21.0
Cr	1.0	23.0
Fe	1.0	25.0
Co	1.0	28.0
Ni	1.0	29.0
Cu	1.0	30.0

[a] H–F from Ref. [5], except C, N, O, Si and P from Ref. [43], Sc–Cu 3*d* parameter from Ref. [15]; All others have been obtained from this work.

as originally suggested by Pople and co-workers [5]. The ultimate justification of Eq. (17) is that such a choice provides a good balance between one- and two-electron terms. A partial theoretical justification comes from the observation that such a choice compensates for the orthogonalization of the basis that lowers the value of two-centred $(\chi_\mu|R_C^{-1}|\chi_\mu)$ from that found over STO's and includes an additional lowering representing the core pseudo-potential necessary to compensate for the inner shell not explicitly considered [45].

3.5. Two-Electron Integrals

The two-electron two-centred non-vanishing integrals γ_{AB} are evaluated over STO's as are the one-centre F^0.

4. The Self-Consistent Field

Equations (6) are generally solved by the Self-Consistent Field (SCF) method that guesses a set of $\boldsymbol{C}^k$, then calculates $\boldsymbol{P}^k$, forms $\boldsymbol{F}^k$, obtains new $\boldsymbol{C}^k$, and repeats this procedure until the energy and $\boldsymbol{P}^k$ have converged to within a specified tolerance. The $\boldsymbol{P}^k$ that is used for the new cycle is generally that obtained from the previous, although various extrapolation procedures have been devised to hasten convergence [30]. For transition metal complexes, the SCF procedure described above seldom succeeds in converging. We have adopted the following procedure that always seems to automatically lead to convergence within the UHF approximation.

A starting set of MO coefficients are generated by diagonalizing a Hückel-like matrix constructed as

$$\begin{aligned} F^0_{\mu\nu} &= -I_{\mu\nu}/2 \\ F^0_{\mu\nu} &= \beta_{\mu\nu} \end{aligned} \tag{18}$$

or $\boldsymbol{F}$ is formed directly from $\boldsymbol{P}^k$ obtained from a previous calculation. To prevent large charge buildup on the transition element and reduce diverging oscillation the $3d$ metal MO's are searched for and their desired occupancy assured. Unless the starting $\boldsymbol{P}^k$ are quite good, this assignment is seldom in order of increasing MO eigenvalue: i.e., the aufbau principle most often leads to divergence. MO's are specified by a threshold value of the AO of interest (usually $3d$) and the phase relation between two or more AOs (symmetry). After two or three cycles of such specification, the occupied orbitals generally stabilize in energy, and, most often, have the lowest orbital eigenvalues. This assignment of orbital occupancies also, of course, allows the calculation of excited states.

The above procedure of electron assignment, by itself, seldom ensures convergence in these complexes. After an extensive investigation [30], we employ a simple "system interaction" method.

Although the prescription given below seems complex, it is based on a very simple idea. Consider a plot of the diagonal elements of the density matrix obtained from diagonalizing $\boldsymbol{F}$, against that assumed to calculate $\boldsymbol{F}$. We wish $\boldsymbol{P}$ (assumed) equal to $\boldsymbol{P}$ (obtained), or $\boldsymbol{P}(a) = \boldsymbol{P}(o)$. Any two successive cycles, say the nth and $(n+1)$st, yields two points, $(P^n(a), P^n(o))$ and $(P^{n+1}(a), P^{n+1}(o))$ on this plot. The intersection of the line connecting these two points, with the 45° line $P(a) = P(o)$ forms the basis of our estimated density for the next cycles; i.e. $\boldsymbol{P}^{n+2}(a) = \boldsymbol{P}^{n+2}(\text{est})$. For simplicity of notation, $\boldsymbol{P}^n$ refers to the nth cycle, and it is understood that the procedure is performed on both α and β spin densities should the system be open-shell.

We obtain the estimated density $\boldsymbol{P}^n(\text{est})$ of the nth cycle from that obtained by solving the secular equation $\boldsymbol{P}^n(o)$ and from $\boldsymbol{P}^{n-1}(a) = \boldsymbol{P}^{n-1}(a) = \boldsymbol{P}^{n-1}(\text{est})$ according to

$$\boldsymbol{P}^n(\text{est}) = \bar{f}\boldsymbol{P}^{n-1}(a) + (1 - \bar{f})\boldsymbol{P}^n(o) \tag{19}$$

with

$$\bar{f} = \sum_{\text{A}} f_{\text{A}} l_{\text{A}}/l \tag{20}$$

where l_{A} is the number of valence basis functions on atom A, l the total number of valence basis functions considered in the sum and

$$f_{\text{A}} = (P^n_{\text{A}}(\text{est}) - P^n_{\text{A}}(o))/(P^{n-1}_{\text{A}}(a) - P^n_{\text{A}}(o))$$

$$P^n_{\text{A}} = \sum_i^{\text{A}} P^n_{ii}. \tag{21}$$

For an orthogonalized set, $P^n_{\text{A}}(o)$ is the number of electrons on atom A, obtained by solving the secular equation (4) assuming $P^{n-1}_{\text{A}}(\text{est})$ in forming $\boldsymbol{F}$; i.e., $F\{P^{n-1}_{\text{A}}(\text{est})\} \rightarrow \{P^n_{\text{A}}(o)\}$. Two successive calculations yield the two points $(P^{n-2}_{\text{A}}(\text{est}), P^{n-1}_{\text{A}}(o))$ and $(P^{n-1}_{\text{A}}(\text{est}), P^n_{\text{A}}(o))$. Assuming a straight line relation exists between these two points, and that we seek the point of intersection with this line and $P^{n-1}_{\text{A}}(\text{est}) = P^{n-1}_{\text{A}}(a) = P^n_{\text{A}}(o)$ for each atom A, gives

$$P^n_{\text{A}}(\text{est}) = [P^n_{\text{A}}(o) - m_{\text{A}}P^{n-1}_{\text{A}}(\text{est})]/(1 - m_{\text{A}})$$

$$m_{\text{A}} = [P^n_{\text{A}}(o) - P^{n-1}_{\text{A}}(o)]/[P^{n-1}_{\text{A}}(\text{est}) - P^{n-2}_{\text{A}}(\text{est})] \tag{22}$$

$$f_{\text{A}} = m_{\text{A}}/(m_{\text{A}} - 1) \tag{23}$$

The following algorithm is adopted:

1. For the first cycle $\boldsymbol{P}^o(a)$ comes from a previous calculation, or the diagonalization of the Hückel matrix of Eq. (18).
2. $\boldsymbol{P}^1(\text{est})$ comes from Eq. (19) assuming $\bar{f} = \frac{1}{2}$.
3. f_{A} is obtained for each atom from Eq. (23) whenever m_{A}, the slope, is negative. For m_{A} positive the intersection of the $P^n_{\text{A}}(\text{est}) = P^{n+1}_{\text{A}}(o)$ line with the line through the two previously obtained points is sensitive to unknown details, and we set $f_{\text{A}} = 0$ (i.e., $P^n_{\text{A}}(\text{est}) = P^n_{\text{A}}(o)$). This is justified as experience shows that $m_{\text{A}} \leqslant 0$ represents all diverging cases met in practice.
4. $\bar{f}$ is formed from Eq. (20) with only atoms with $m_{\text{A}} \leqslant 0$ included in the sum.
5. Steps 3 to 5 are repeated until the desired convergence is obtained. Most often

$\bar{f} \to 0$, representing the usual SCF procedure is obtained after close convergence. When $\bar{f}$ does not approach zero the convergence is not stable, and the single determinant description of the state forced to convergence is often not adequate.

For comparison, we have tried this procedure or similar ones, to estimate each element of the density matrix separately, each diagonal element separately (with renormalization of off-diagonal terms), for each atom separately, and finally, the entire system as described above [30]. The last procedure appears the best, and has the advantage that Eq. (19) yields a $\boldsymbol{P}^n(\text{est})$ such that Trace $\boldsymbol{P} = N$. We have also tried simple level shifting procedures, which, although effective, require more time per cycle.

5. Spin Projection

The eigenfunctions of the unrestricted Hartree–Fock procedure are not necessarily eigenfunctions of the spin operator S^2 [46]. Rather

$$\langle \Psi^{\text{uhf}} | S^2 | \Psi^{\text{uhf}} \rangle \equiv \langle S^2 \rangle_{\text{uhf}} = s'(s' + 1) + q - \operatorname{Tr}(P^\alpha P^\beta) \tag{24}$$

with $s' = s_z = (p - q)/2$, one half the number of α electrons, p, minus the number of β electrons, q.

In practice the amount of spin "contamination" in most cases is very small, and we have adopted a simple spin annihilation to purify the state [47]. The amount of algebra involved in a simple annihilation is considerably less than that involved in a complete spin projection.

We define the annihilator $A_{s'+1}$ as

$$A_{s'+1} \equiv S^2 - (s' + 1)(s' + 2).$$

Then

$$\begin{aligned}
\Psi^{\text{uhf}} &= \sum_{s=s'} C_s \Psi_s \\
S^2 \Psi_s &= s(s + 1)\Psi_s \\
A_{s'+1}\Psi^{\text{uhf}} &= \sum_{s=s'} C_s \{s(s + 1) - (s' + 1)(s' + 2)\}\Psi_s \\
&= -2(s' + 1)C_{s'}\Psi_{s'} + 2(s' + 2)C_{s'+2}\Psi_{s'+2} + \cdots
\end{aligned} \tag{25}$$

This yields

$$\begin{aligned}
\langle S^2 \rangle_{aa} &= \frac{\langle A_{s'+1}\Psi^{\text{uhf}} | S^2 | A_{s'+1}\Psi^{\text{uhf}} \rangle}{\langle A_{s'+1}\Psi^{\text{uhf}} \mid A_{s'+1}\Psi^{\text{uhf}} \rangle} \\
&= \frac{\langle S^6 \rangle_{\text{uhf}} - 2(s' + 1)(s' + 2)\langle S^4 \rangle_{\text{uhf}} + (s' + 1)^2(s' + 2)^2\langle S^2 \rangle_{\text{uhf}}}{\langle S^4 \rangle_{\text{uhf}} - 2(s' + 1)(s' + 2)\langle S^2 \rangle_{\text{uhf}} + (s' + 1)^2(s' + 2)^2}
\end{aligned} \tag{26}$$

with $\langle S^2 \rangle_{\text{uhf}}$ given in Eq. (24) and $\langle S^4 \rangle_{\text{uhf}}$ and $\langle S^6 \rangle_{\text{uhf}}$ given in Ref. [47], Eqs. (44)–

(46), with "A" of that reference defined as $s'(s' + 1) + q$. After annihilation, the densities are approximated by

$$\begin{aligned} \boldsymbol{P}^{\alpha}_{aa} &= \boldsymbol{P}^{\alpha} - 2\{\boldsymbol{P}^{\alpha}\boldsymbol{P}^{\beta}\boldsymbol{P}^{\alpha} - (\boldsymbol{P}^{\alpha}\boldsymbol{P}^{\beta} + \boldsymbol{P}^{\beta}\boldsymbol{P}^{\alpha})/2\}/X \\ \boldsymbol{P}^{\beta}_{aa} &= \boldsymbol{P}^{\beta} - 2\{\boldsymbol{P}^{\beta}\boldsymbol{P}^{\alpha}\boldsymbol{P}^{\beta} - (\boldsymbol{P}^{\beta}\boldsymbol{P}^{\alpha} + \boldsymbol{P}^{\alpha}\boldsymbol{P}^{\beta})/2\}/X \\ X &= 2s' + 2 - q + \mathrm{Tr}\,(\boldsymbol{P}^{\alpha}\boldsymbol{P}^{\beta}). \end{aligned} \tag{27}$$

The above equations are derived from analysis of Eq. (25) that yield

$$\begin{aligned} \langle\ \rangle_{aa} &= 2\langle\ \rangle_{asa} - \langle\ \rangle_{\text{uhf}} + \theta\left\{\frac{(C_{s+1})^2}{(C_s)}, \frac{C_{s+2}}{C_s}\right\} \\ \langle\ \rangle_{asa} &\equiv \langle\Psi^{\text{uhf}}|\ |A_{s'+1}\Psi^{\text{uhf}}\rangle/\langle\Psi^{\text{uhf}}\ |\ A_{s'+1}\Psi^{\text{uhf}}\rangle \end{aligned} \tag{28}$$

and dropping terms of order $(C_{s+1}/C_s)^2$ and (C_{s+2}/C_s) or smaller. Equations (27) are similar to those obtained by Amos and Hall for a single-sided annihilation, $\langle\ \rangle_{asa}$, except for the factor of two multiplying the second term of $\boldsymbol{P}^{\alpha}_{aa}$ and $\boldsymbol{P}^{\alpha}_{aa}$ [48]. The spin density is then given by

$$\rho = \boldsymbol{P}^{\alpha}_{aa} - \boldsymbol{P}^{\beta}_{aa} \simeq \boldsymbol{P}^{\alpha} - \boldsymbol{P}^{\beta} - (\boldsymbol{P}^{\alpha}\boldsymbol{P}^{\beta}\boldsymbol{P}^{\alpha} - \boldsymbol{P}^{\beta}\boldsymbol{P}^{\alpha}\boldsymbol{P}^{\beta})/X. \tag{29}$$

In general, $\boldsymbol{P}^{\alpha}_{aa} \simeq \boldsymbol{P}^{\alpha}$ and $\boldsymbol{P}^{\alpha}_{aa} \simeq \boldsymbol{P}^{\beta}$ and dropping the higher order terms in Eq. (27) seems empirically justified. The spin density, however, magnifies these deficiencies, and Eq. (29) is not valid for calculating excited states when S_z is not equal to its maximum value; i.e., when $C_{s+1}/C_s \simeq 1$.

Examining the energy in somewhat greater detail we find

$$W_{asa} = \langle\Psi^{\text{uhf}}|H|A_{s'+1}\Psi^{\text{uhf}}\rangle = W_{\text{uhf}} - Q/2X \tag{30}$$

with Q given by

$$\begin{aligned} Q = 2\,\mathrm{Tr}\,&(\boldsymbol{P}^{\alpha}\boldsymbol{P}^{\beta}\boldsymbol{P}^{\alpha} + \boldsymbol{P}^{\beta}\boldsymbol{P}^{\alpha}\boldsymbol{P}^{\beta} - 2\boldsymbol{P}^{\alpha}\boldsymbol{P}^{\beta})H \\ &+ \sum_{ijkm}\{(\boldsymbol{P}^{\alpha}\boldsymbol{P}^{\beta}\boldsymbol{P}^{\alpha} + \boldsymbol{P}^{\beta}\boldsymbol{P}^{\alpha}\boldsymbol{P}^{\beta} - 2\boldsymbol{P}^{\alpha}\boldsymbol{P}^{\beta})_{mi}(\boldsymbol{P}^{\alpha} + \boldsymbol{P}^{\beta})_{jk} \\ &\qquad + (\boldsymbol{P}^{\alpha} - \boldsymbol{P}^{\alpha}\boldsymbol{P}^{\beta})_{ji}(\boldsymbol{P}^{\alpha}\boldsymbol{P}^{\beta} - \boldsymbol{P}^{\beta})_{mk} - (\boldsymbol{P}^{\alpha}\boldsymbol{P}^{\beta}\boldsymbol{P}^{\alpha})_{ji}\boldsymbol{P}^{\beta}_{mk} \\ &\qquad - (\boldsymbol{P}^{\beta}\boldsymbol{P}^{\alpha}\boldsymbol{P}^{\beta})_{ji}\boldsymbol{P}^{\beta}_{mk} + (\boldsymbol{P}^{\alpha}\boldsymbol{P}^{\beta})_{ji}(\boldsymbol{P}^{\alpha} + \boldsymbol{P}^{\beta})_{mk}\}(im\mid jk). \end{aligned} \tag{31}$$

Equation (28) for the energy correct up to order $(C_{s+1}/C_s)^2$ is

$$\begin{aligned} W_{aa} &= 2W_{asa} - W_{\text{uhf}}/C^2_{s'} + (C_{s'+1}/C_{s'})^2E_{s'+1} \\ E_{s'+1} &= \langle\Psi_{s'+1}|H|\Psi_{s'+1}\rangle/\langle\Psi_{s'+1}\mid\Psi_{s'+1}\rangle. \end{aligned} \tag{32}$$

Writing $E_{s'+1} = W_{\text{uhf}} + \delta$ yields

$$W_{aa} = W_{\text{uhf}} - Q/X + (C_{s'+1}/C_{s'})^2\delta. \tag{33}$$

We will ignore the last term of Eq. (33) and use

$$W_{aa} = W_{\text{uhf}} - Q/X \tag{34}$$

which is computationally very rapid. Since $\delta \simeq W_{aa} - W_{\text{uhf}}$, the relative error introduced into the correction by such a truncation is $(C_{s'+1}/C_{s'})^2$, which is usually less than 1%. (For the chlorides of the next section, the error is of the order of 5×10^{-6} a.u.) Again, the exception is met when calculating states in which S_z is not its maximum value for the given number of open shells.

Equation (34) is most rapidly evaluated using Eqs. (27). This yields

$$W_{aa} = (\mathrm{Tr}\,(\boldsymbol{P}^{\alpha}_{aa} + \boldsymbol{P}^{\beta}_{aa})H + \mathrm{Tr}\,\boldsymbol{P}^{\alpha}_{aa}\boldsymbol{F}^{\alpha} + \mathrm{Tr}\,\boldsymbol{P}^{\beta}_{aa}\boldsymbol{F}^{\beta})/2 + Y$$

$$Y = -\left\{\sum_{ijkm} (\boldsymbol{P}^{\alpha} - \boldsymbol{P}^{\alpha}\boldsymbol{P}^{\beta})_{ji}(\boldsymbol{P}^{\alpha}\boldsymbol{P}^{\beta} - \boldsymbol{P}^{\beta})_{mk}(im \mid jk)\right\}\Big/ X. \tag{35}$$

In general, Y is small.

Making use of Eqs. (25), we derive

$$C^2_{s+1} = (\langle S^2\rangle_{\mathrm{uhf}} - \langle S^2\rangle_{aa})/2(s+1)$$

$$C^2_{s+2} = (\langle S^2\rangle_{aa} - \langle S^2\rangle_{asa})(1 - C^2_{s+1})/4(2s+3). \tag{36}$$

In the expressions above, terms of order $(C_{s+3}/C_{s+2})^2$ and higher have been dropped. Equations (35) are used to check the validity of Eqs. (34), (29) and (27).

6. Some Results

The present model and associated computer programs have been in use for over two years [30] by several groups. The results obtained are good when compared to *ab initio* calculations or to experiment. Calculations on the spectra of transition metal complexes [49, 50][1] seem to be in excellent accord with experiment. We wish in this paper only to present some results on the chlorides of Fe, Cu and Co, and to compare these results to those obtained by other types of calculations, and to experiment.

6.1. *Iron Chloride* $FeCl_4^{-1}$

$FeCl_4^{-1}$ is a tetrahedral complex with a bond length of 2.1955 Å [51]. As is usual with T_d complexes the molecule is of high spin, in this case with five unpaired electrons.

Calculations were performed at the experimental bond length and are reported in Table 6, along with the unrestricted X_α SW results of Noodleman [52]. The orbital energies for the MO's with both the α and β components occupied agree fairly well with the X_α results, but the energies of the α $3e$ and $10t_2$ MO's which have no occupied β counterpart are 0.54 and 0.60 a.u., respectively, below the X_α results. These orbitals are the principal $3d$ metal MO's (the $7t_2$ MO is taken as a ligand $3s$ orbital despite the high metal $3d$ character). In our results the $3d$ MO's are not the HOMO's but lie well below the ligand $3p$ MO's. This feature is characteristic of many Hartree–Fock calculations (for example, the following section on $CuCl_4^{-2}$).

---

[1] Ref. [50] is a comprehensive study of the excited states of $CuCl_2$ using the methods presented in this paper along with *ab initio* ΔE and CI calculations, and scattered wave $X\alpha$ calculations.

Table 6. $FeCl_4^{-1}(T_d)$ results (a.u.)

	Noodleman [96] X_α S.W.			This work INDO/1		
	ε_i		Nature	ε_i		
	α	β		α	β	average
$10t_2(3d)$[a]	−0.193		Fe 3*d*	−0.681(50)[a]	[+0.126][b](69)[a]	−0.282(58)[a]
$3e(3d)$[a]	−0.218		Fe 3*d*	−0.747(98)[a]	[+0.226][b](96)[a]	−0.260(97)[a]
$2t_1$	−0.242	−0.234	Cl 3*p*	−0.303	−0.282	−0.292
$9t_2$	−0.279	−0.265	Cl 3*p* + Fe 3*d*	−0.275	−0.316	−0.295
$2e$	−0.302	−0.270	Cl 3*p* + Fe 3*d*	−0.307	−0.311	−0.309
$8t_2$	−0.331	−0.300	Cl 3*p* + Fe 3*d*	−0.351	−0.336	−0.343
$8a_1$	−0.341	−0.328	Cl 3*p* + Fe 3*d*	−0.362	−0.306	−0.334
$7t_2$	−0.710	−0.700	Cl 3*s*	−0.827(49)[a]	−0.739	−0.783
$7a_1$	−0.721	−0.722	Cl 3*s*	−0.804	−0.776	−0.790
Atomic charges:						
Cl					−0.406	(−0.664)[e]
Fe					+0.624	(+1.654)[e]
Metal orbital populations:						
3*d*					5.957	(5.951)[e]
4*s*					0.457	(0.181)[e]
4*p*					0.963	(0.214)[e]

[a] Percentage metal 3*d* character.

[b] The β 3*e* and $10t_2$ MO's are unoccupied.

[e] Mulliken population analysis.

The X_α SW one electron energies are obtained using Slater's transition state theory [53], in which half an electron is withdrawn from each orbital in turn. Thus each value is obtained from a separate calculation, and corresponds directly to an ionization potential (IP); that is, to the energy required to remove an electron from "a given orbital" and includes in an average way the reorganization of the system upon ionization. This approach seems to yield the classical MO picture with the metal 3*d* MO's as HOMO's. This classical picture of transition metal orbitals has evolved as one generally thinks in terms of orbitals which obey Koopmans' approximation when assigning the negative of orbital energies to ionization processes.

As we have used the UHF procedure, the calculated eigenvalues are "orbital energies" in the sense that they obey Koopmans' approximation; that is, in the *absence* of molecular relaxation (the reorganization of the other $2n - 1$ (or $2n$) electrons) upon the loss (or gain) of an electron they represent ionization potentials (or electron affinities). However, *ab initio* calculations demonstrate that the relaxation for the loss of a "3*d* electron" is 0.3–0.5 a.u., which should be added to the Koopmans potential to give an estimate of the IP. Assuming 0.4 a.u. is a typical value of the relaxation for the removal of an electron from a MO of principally metal 3*d* character places our IP estimates in reasonable accord with the X_α one-electron energies. Such a blanket estimate of the relaxation, however, must be

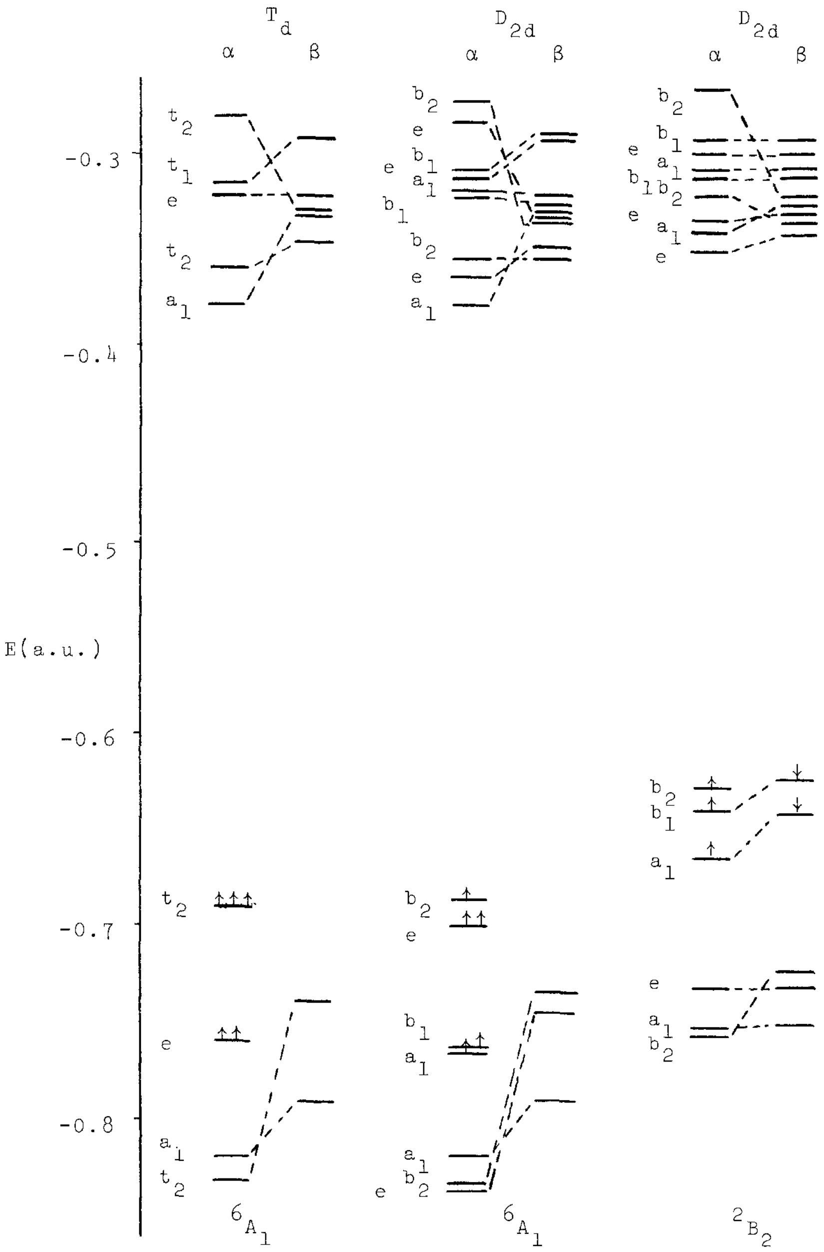

Fig. 1. Molecular orbital diagram for $FeCl_4^{-1}$. ↑ indicates the half filled Fe "3*d*" MO's. All orbitals shown in the figure are occupied

viewed with caution, and the direct estimate of more accurate IP's from a single calculation will be difficult.

One method which may prove useful in the estimation of some ionization energies involves averaging the energies of an appropriate pair of α and β spin orbitals. When only the α spin orbital is occupied, as is the case for the metal $3d$ orbital(s), the averaging corresponds to an average of an ionization potential and an electron affinity. We can, however, view this average in a different fashion. Consider a doublet. The removal of an unpaired α electron corresponds to an ionization process. If we replace this electron in the corresponding β orbital we should recover the other degenerate component of the doublet. The energy to do this, $-\varepsilon_i^\alpha$ (occupied) + ε_i^β (unoccupied), should be zero, but it will not because of relaxation. We define $2R$ as the amount of relaxation necessary to give a net change of energy equal to zero. That is,

$$M(^2\Gamma_{1/2}) \rightarrow M^+(^1\Gamma_0) \rightarrow M(^2\Gamma_{-1/2}) - \varepsilon_i^\alpha(\text{occ}) + \varepsilon_i^\beta\,(\text{unocc}) + 2R = 0$$

$$R = \tfrac{1}{2}(\varepsilon_i^\alpha(\text{occ}) - \varepsilon_i^\beta(\text{unocc}))$$

where $^{2s+1}\Gamma_{sz}$ labels the states of molecule M. If we then assume that the relaxation energy for the loss of an electron is equal to that for the gain of an electron, then

$$\text{IP}_i = -\varepsilon_i^\alpha(\text{occ}) + R = -\tfrac{1}{2}(\varepsilon_i^\alpha(\text{occ}) + \varepsilon_i^\beta(\text{unocc})) \equiv \varepsilon_i(\text{ave}).$$

This is a crude approximation, and it becomes even more so when the molecule is not a doublet as the final and starting molecular species are then of different spin multiplicities. This approach does, however, restore the classical picture with the metal $3d$ MO as HOMO when the corresponding β metal orbitals are unoccupied. In this particular case, this approach leads to a reversal of the metal e and t_2 orbitals. While this averaging procedure is unlikely to yield accurate estimates of IP's when relaxation is important, it does allow for a better estimate than do the individual eigenvalues.

In cases where accuracy is required, it will be necessary to carry out separate calculations for each electronic configuration corresponding to an ionization process in order to determine the total energy, and thus the change in total energy. This process is found to work well provided the calculations on M and M^+ are of the same quality. There is some question of the accuracy of such a subtraction of such large numbers when both calculations are not of the restricted HF type.

We have carried out calculations on $FeCl_4$ using a slightly distorted molecule of D_{2d} symmetry to avoid symmetry breaking. For the high spin $FeCl_4^{-1}$ molecule we calculate that the lowest IP results from the removal of an α electron from a b_2 MO that is principally ligand in nature, Table 7. The ΔE_{SCF} value is 0.269 a.u. which corresponds well to the Koopmans' potential of $-\varepsilon_{b_2}^\alpha(\text{occ}) = 0.275$ a.u., or $-\varepsilon_{b_2}(\text{ave}) = 0.299$ a.u. for $FeCl_4^{-1}$ or $-\varepsilon_{b_2}^\alpha(\text{unocc}) = 0.266$ a.u. for $FeCl_4$, indicating that there is little relaxation for this ionization process. We also attempted to remove the unpaired α electron from the metal b_2 MO but we were not able to keep this state from mixing with the previously calculated state.

In order to examine further the order of the energies for the ionization processes b_2(ligand) $<$ b_2(metal), we have also calculated the energies of a series of low spin configurations of $FeCl_4$. The calculated ΔE_{SCF} values are given in Table 7 along with the results of the low spin $FeCl_4^{-1}$ molecule. The removal of an electron from the b_2 MO of ligand character appears to require less energy than the removal of the unpaired $3d$ electron, Fig. 2. The relaxation involved in the removal of the "$3d$" electron is 0.345 a.u., a value in good accord with the estimates from *ab initio* results, and in reasonable accord with the value inferred from ε(ave).

When the energies of high and low spin $FeCl_4^{-1}$ systems in the distorted tetrahedral geometry, Fig. 1, are compared, the high spin configuration is more stable by 0.081 a.u. or 2.20 eV. For the tetrahedral $FeCl_4^{-1}$ system we calculate an equilibrium bond length of 2.242 Å which compares well with the experimental length of 2.1955 Å. The expectation value of S^2 before annihilation of the next highest spin component of the high spin complex is 8.753297, after, 8.750002. The annihilation lowers the SCF energy by 0.0002 a.u.

6.2. *Copper Chloride* $CuCl_4^{-4}$

The calculations were carried out on the square planar geometry (D_{4h}) using a Cu–Cl bond length of 2.26 Å, which is an average of the reported experimental values for the square planar configuration, 2.30 Å [55], and the tetrahedral one, 2.22 Å [56]. Comparison is made with the restricted *ab initio* results of Veillard *et al.* [54] and the "revised INDO" results of van der Lugt [14]. This was one of the first

Table 7. Low spin $FeCl_4^{-1}(D_{2d})$ results (a.u.)

	ε_i			
	α	β	average	ΔE_{SCF}(state)
$4b_2(xy)$[a]	$-0.625(66)$[a]	$[+0.199]$[b](78)[a]	-0.213	0.280 ($^1A_1$)
$3b_2$	-0.256	-0.317	-0.287	0.269 ($^1A_1$)
				0.304 ($^3A_1$)
$3b_1$	-0.292	-0.294	-0.293	0.31 ± 0.01($^1A_2$)
				0.30 ± 0.01($^3A_2$)
$4e$	-0.297	-0.296	-0.297	
$2b_1$	-0.301	-0.303	-0.302	
$4a_1$	-0.302	-0.301	-0.302	
$3e$	-0.332	-0.325	-0.329	
$2b_2$	-0.332	-0.344	-0.338	
$3a_1$	-0.347	-0.344	-0.346	
$2e$	-0.362	-0.351	-0.357	
$1b_1(x^2-y^2)$[a]	$-0.632(97)$[a]	$-0.618(96)$[a]	-0.625	
$2a_1(z^2)$[a]	$-0.662(97)$[a]	$-0.636(97)$[a]	-0.649	
$1e$	-0.756	-0.754	-0.755	
$1b_2$	-0.779	-0.743	-0.761	
$1a_1$	-0.799	-0.798	-0.799	

[a] Percentage metal $3d$ character.

[b] The β $4b_2$ MO is unoccupied.

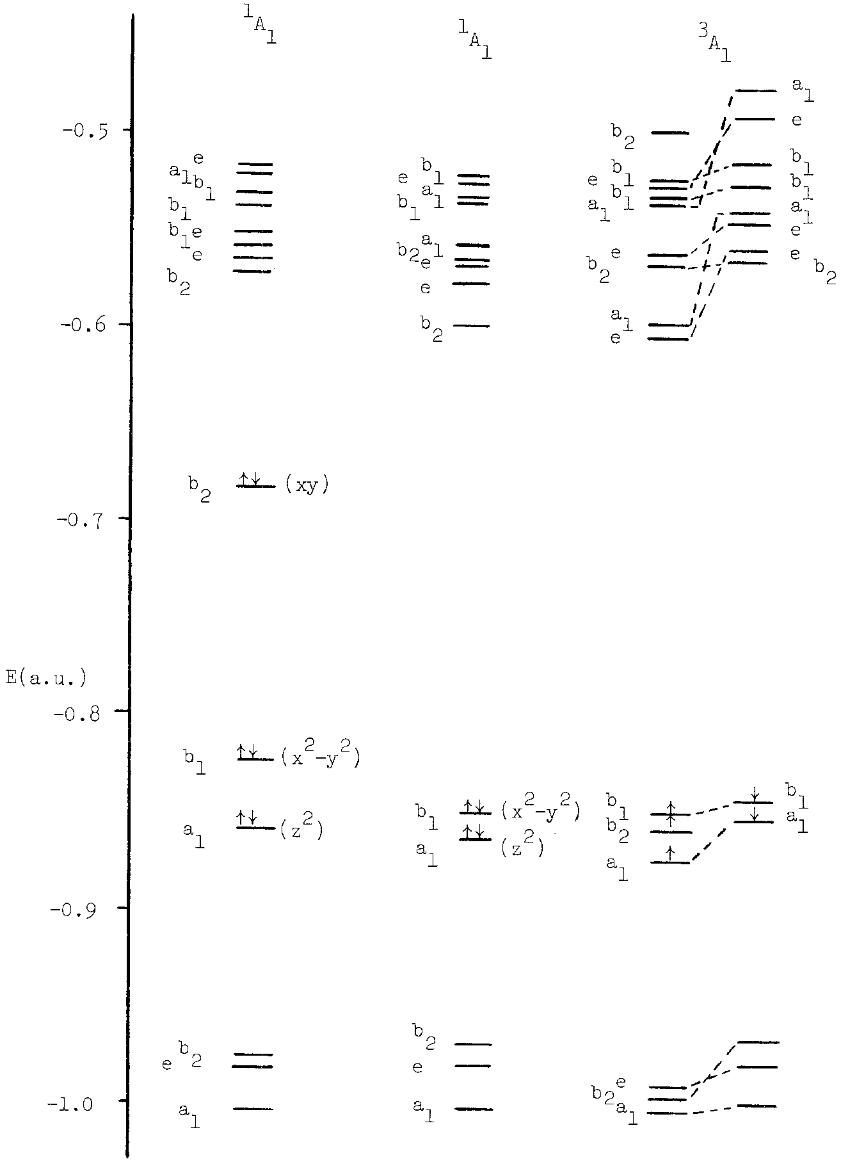

Fig. 2. Molecular orbital diagram for $FeCl_4$ (D_{2d}). ↑ indicates the half filled Fe "3*d*" MO's. All other orbitals of the figure are occupied

systems for which a Hartree–Fock calculation yielded the metal 3*d* orbitals firmly below the ligand 3*p* [57]. An earlier Extended Hückel calculation [58] on this ion had put the metal 3*d* orbitals in the typical ligand field position as the HOMO's.

The results of the three methods are reported in Table 8. Two *ab initio* calculations are presented: the enlarged Basis III yielding a total energy of −3472.284 a.u. and

Table 8. $CuCl_4^{-2}$ results (a.u.)

	Ab initio [54] (restricted)		"Revised"	This work INDO/1		
	Basis *III*	Basis *II*	INDO [14]	α	β	average
$6b_{1g}(d_{x^2-y^2})$	−0.461[a](96)[b]	−0.476[a]	−0.24[c](49)[b]	−0.540(73)[b]	+0.422[d](70)[b]	−0.059(72)[b]
$2s_{2g}$	−0.055	−0.065(−0.067)[e]	−0.12	−0.029	−0.026	−0.027
$9e_u$	−0.084	−0.091	−0.08	−0.040	−0.028	−0.034
$2b_{2u}$	−0.091	−0.099(−0.101)[e]	−0.14	−0.054	−0.051	−0.053
$3e_g$	−0.109	−0.112	−0.14	−0.055	−0.052	−0.054
$4a_{2u}$	−0.130	−0.139(−0.141)[e]	−0.18	−0.075	−0.072	−0.073
$3b_{2g}$	−0.140	−0.150(−0.152)[e]	−0.16	−0.085	−0.082	−0.083
$5b_{1g}$	−0.141	−0.163	−0.05	+0.022	−0.061	−0.020
$8e_u$	−0.157	−0.165	−0.16	−0.127	−0.106	−0.117
$9a_{1g}$	−0.188	−0.197(−0.218)[e]	−0.17	−0.117	−0.095	−0.106
$8a_{1g}(d_{z^2})$	−0.447(96)[b]	−0.465(−0.528)[e]	−0.43(100)[b]	−0.417(88)[b]	−0.391(90)[b]	−0.404(89)[b]
$2e_g(d_{xz}, d_{yz})$	−0.463(98)[b]	−0.482	−0.44(100)[b]	−0.436(99)[b]	−0.411(99)[b]	−0.423(99)[b]
$2b_{2g}(d_{yz})$	−0.504(98)[b]	−0.522(−0.553)[e]	−0.47(100)[b]	−0.457(99)[b]	−0.443(99)[b]	−0.450(99)[b]
$4b_{1g}$	−0.644		−0.58	−0.400	−0.435	−0.418
$7e_u$	−0.660		−0.68	−0.522	−0.509	−0.516
$7a_{1g}$	−0.683		−0.72	−0.566	−0.551	−0.559
Atomic charges						
Cl	(−0.88)[f]	(−0.91)[f]	−0.473	−0.605(−0.823)[f]		
Cu	(+1.54)[f]	(+1.62)[f]	−0.109	+0.420(+1.290)[f]		
Metal orbital populations						
3*d*	(9.08)[f]	(9.07)[f]	9.532	9.291(9.288)[f]		
4*s*	(0.10)[f]	(0.09)[f]	0.629	0.461(0.250)[f]		
4*p*	(0.28)[f]	(0.22)[f]	0.948	0.825(0.169)[f]		

[a] As the methods are restricted, the energies of the open-shell orbitals are not directly comparable to those of the closed-shell orbitals, see text.

[b] Percentage of metal 3*d* character.

[c] The $6b_{1g}$ eigenvalue −0.03 of the revised INDO calculation must be corrected by $J_\infty/2$ to be compared with the *ab initio* results, see Ref. [14].

[d] The $6b_{1g}$ β MO is unoccupied.

[e] The closed-shell orbital eigenvalues are corrected by $3/2K$ to give the Koopmans' potential, see [54].

[f] The Mulliken population analysis is given in parentheses.

Basis II yielding -3470.577 a.u. A comparison of orbital eigenvalues, however, indicates that they have stabilized with respect to improvements of the basis set. As the *ab initio* calculations are restricted, Koopmans' theorem applies only to the open shell eigenvalues. The closed shell eigenvalues must be corrected by exchange terms before the orbitals correspond to "Koopmans' orbitals". These adjusted values have been estimated for Basis II and are reported in parentheses in Table 8. For the MO's of ligand character this correction is quite small, and for the MO's of metal character the correction is 0.06 a.u. or less. As the unrestricted formalism directly yields Koopmans' orbitals, our eigenvalues should be compared with the RHF open-shell eigenvalues and the closed-shell eigenvalues corrected for exchange. Since this exchange correction appears small, a direct comparison is not invalid. The eigenvalues obtained from the "revised INDO" model of van der Lugt need all be corrected for this comparison, but only the correction for the open-shell $6b_{1g}$ orbital is sizeable, and this has been made in the table.

The results of all three calculations are reasonably similar. There are four low-lying orbitals, $7a_{1g}$, $7e_u$, and $4b_{1g}$, that are principally Cl 3*s*. Both the approximate calculations predict the splitting of these orbitals to be too large at about 0.14 a.u. compared to the *ab initio* result of 0.04 a.u. This is a common fault in most of our calculations and is caused by too large an interaction between the metal 4*s* and the ligand AO's. In addition, our results suggest that these Cl 3*s* orbitals are interspersed with the occupied metal orbitals, Fig. 3, whereas the other two suggest a separation of about 0.1 a.u. This has been caused by a mixing of 3*d* into both the $4b_{1g}$ and $6b_{1g}$ orbitals in the UHF calculation, Table 8. In the *ab initio* results the metal orbitals are split by about 0.08 a.u. with the $6b_{1g}(d_{x^2-y^2})$ orbital lying highest in energy only after the exchange correction is made to the closed-shell orbital energies. Our calculated splitting of the metal orbitals is about 0.12 a.u. with the $6b_{1g}$ orbital lying lowest in energy. This also seems to be a feature of the UHF calculation rather than the model [50]. The splitting of 0.23 a.u. as calculated by the "revised INDO" model is probably too large, although such a conclusion is not certain until a dependent observable is calculated.

In all calculations four doubly occupied orbitals, or their counterparts in the UHF calculation, can be classified as nearly pure metal orbitals. The singly occupied $6b_{1g}$ MO is nearly pure metal in the *ab initio* results, 73% in our results, and only 49% in the "revised INDO" results. The *ab initio* and the INDO/1 results then show a gap of about 0.25 a.u. before the onset of 12 MO's that are principally Cl 3*p*. The "revised INDO" results show a smaller gap of about 0.07 a.u. before the onset of these MO's. This discrepancy arises from the position of the $6b_{1g}$ orbital of that calculation.

In comparing the results of a Mulliken population analysis it can be seen, Table 8, that our atomic charges are in good agreement with those obtained from the *ab initio* calculation using Basis III [59]. The balance of 4*s* and 4*p*, however, is not the same. The calculation of a negative charge for the Cu atom in the "revised INDO" results is not in agreement with our results, and indicates less metal back-bonding to the ligands. A direct comparison between the "revised INDO" results

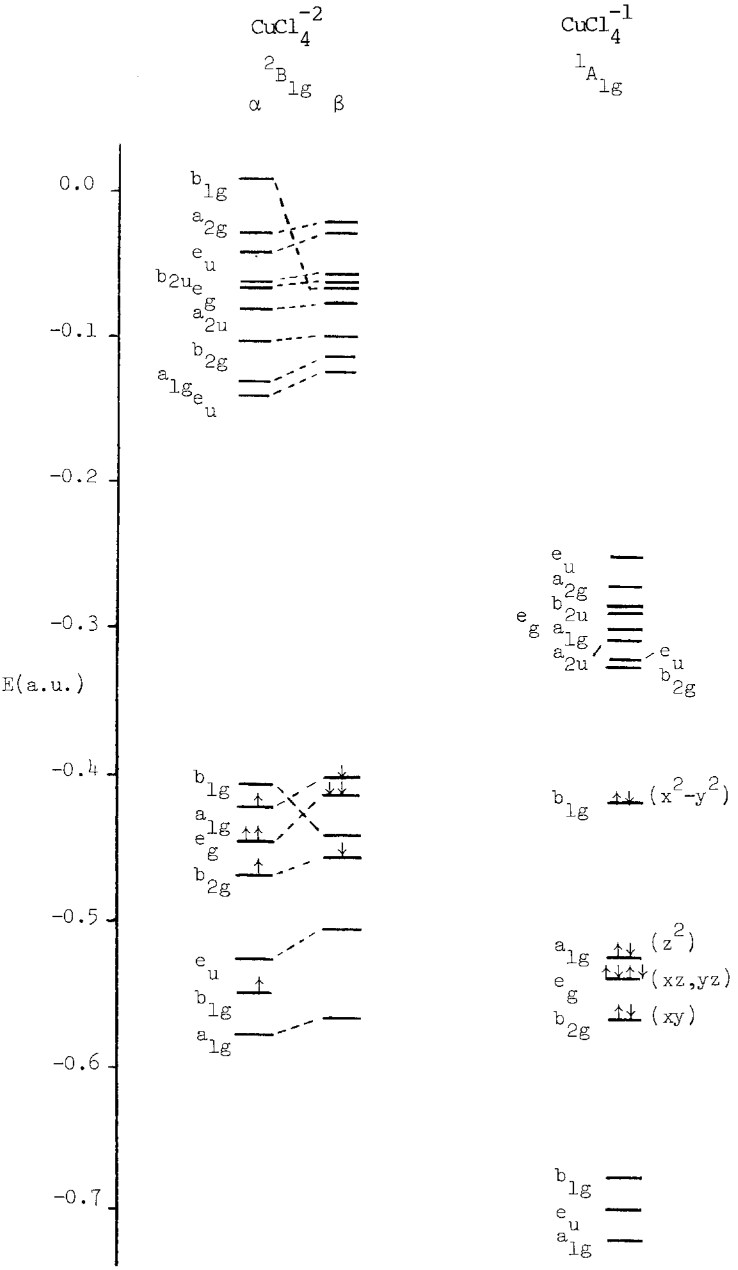

Fig. 3. Molecular orbital diagram for $CuCl_4^{-2}$ and $CuCl_4^{-1}$. ↑ indicates the Cu "3*d*" orbitals. All other orbitals of the diagram are occupied

and the *ab initio* results cannot be made, as the former refers to the charge calculated directly from the Fock–Dirac density over an orthogonalized basis [59].[2]

In all these calculations there are two notable features in the ordering of the orbitals, all of which should obey (neglecting relaxation), or nearly obey, Koopmans' approximation. The first of these is the fact that the ligand $3p$ orbitals lie above the metal $3d$ orbitals; the second, that there is a singly occupied $6b_{1g}$ MO below many of the doubly occupied levels. Neither result can be considered as "conventional". The first apparent contradiction in light of Koopmans' approximation has been discussed in terms of the relaxation energy. Even so, as the net charge on each of the Cl atoms is calculated to be nearly -1 from either the *ab initio* or INDO/1 results, the loss of an electron from orbitals localized on the ligands is an attractive alternative to the loss of an electron from an already positively charged Cu atom. The second feature of a singly occupied orbital lying up to 0.4 a.u. below other doubly occupied levels can be understood from an examination of two electron terms. If the energy involved in the removal of an electron from the HOMO were the same as that required to pair two electrons in the $6b_{1g}$ MO, then the net gain in energy would be the eigenvalue difference (this neglects changes in the exchange energy, but this should be small), making the process favoured. However, the Coulomb repulsion between two electrons in the HOMO, which is a very delocalized orbital, is unlikely to be greater than 0.2–0.3 a.u., while the Coulomb repulsion between two electrons in the $6b_{1g}$ MO, which is nearly pure metal and thus very localized, is about 1.0 a.u. Thus the process is not favoured and the $6b_{1g}$ MO remains singly occupied in spite of the low eigenvalue.

The fact that the $6b_{1g}$ MO has the lowest energy of the "metal $3d$" orbitals in our results and yet is the singly occupied orbital rather than, say, the $8a_{1g}(d_{z^2})$ with a higher energy suggests that the easiest metal orbital to remove an electron from is the $6b_{1g}$; that is, that the relaxation for the removal of the electron from the $6b_{1g}$ orbital is somewhat larger than the relaxation from the other metal-like MO's. Thus, although our eigenvalue ordering is

$$d_{x^2-y^2} < d_{xy} < d_{xz}, d_{yz} < d_{z^2}$$

the very presence of the hole in the $d_{x^2-y^2}$ MO suggests that the electrons are removed in order of ease

$$d_{xy} < d_{xz}, d_{yz} < d_{z^2} < d_{x^2-y^2}$$

This is in agreement with the order suggested by Figgis [60] to account for the magnetic and spectral properties of square planar complexes, and with the corrected eigenvalue ordering of the restricted calculations of Veillard *et al.* and the ordering obtained by van der Lugt.

---

[2] For this comparison we assume that our basis is a Löwdin symmetrical orthogonalized one, and make the transformation back to Slater type orbitals. The justification for such an assumption, however, is weak, and we view the results of the Mulliken population analysis with some reservations; see, e.g. Ref. [17].

Table 9. Ionization potentials of $CuCl_4^{-2}$ from ΔE_{SCF} calculations (a.u.)

Electron removed	State	ΔE_{SCF}	$-\varepsilon_i$(occ)	$-\varepsilon_i$(ave)
b_{1g}(ligand)	$^1A_{1g}$	−0.014	−0.022	0.020
b_{1g}(ligand)	$^3A_{1g}$	0.048	0.061	0.020
a_{2g}(ligand)	$^1B_{2g}$	0.032	0.029	0.027
a_{2g}(ligand)	$^3B_{2g}$	0.025	0.026	0.027

The ΔE_{SCF} values for the removal of an electron from the $5b_{1g}$ and $2a_{2g}$ MO's which are of ligand character are given in Table 9. These values compare quite well with the $-\varepsilon_i$ (occ) values indicating that the relaxation for the removal of an electron from an orbital of ligand character is again small. The ΔE_{SCF} value of 0.039 a.u. for the removal of an electron from the $2a_{2g}$ ligand MO is in good accord with the *ab initio* result of 0.056 a.u. We were unable to calculate the energy of the $^1A_{1g}$ state corresponding to the removal of the unpaired electron from the $6b_{1g}$ MO. The *ab initio* calculation did not have this difficulty for this particular b_{1g} MO, and Veillard *et al.* report an IP of 0.110 a.u.

In both the *ab initio* and INDO/1 results the lowest IP is due to the loss of an electron from a molecular orbital which is principally ligand in nature, Fig. 3. Upon the loss of an electron from a "*d* MO", sizeable relaxation is found and IP's of about 0.1 a.u. are estimated. Thus, even though the difference between the ligand and metal orbital eigenvalues is large, the estimated differences of IP's are quite small making it difficult to order the ionization processes from these calculations. An interesting feature of the *ab initio* ΔE_{SCF} calculations, in contrast to the exchange corrected MO eigenvalue ordering, is that the loss of an electron from the $2b_{2g}(d_{xy})$ orbital appears to require less energy than the removal of the unpaired electron from the $6b_{1g}$ orbital. This implies a reversal of our usual concepts of the metal orbital ordering in a D_{4h} ligand field, but the difference is sufficiently small (0.007 a.u.) that it may well be a result of the mechanics of the calculation, rather than a real result.

For the equilibrium bond length of the D_{4h} system we calculate a value of 2.255 Å which compares very well with the experimental values of 2.30 Å given for $(NH_4)_2CuCl_4$ [55] and 2.265 Å given for $[(C_6H_5)CH_2CH_2CH_3]_2CuCl_4$ [61]. For the distorted tetrahedral complex we calculate a bond length of 2.260 Å, to be compared with values ranging from 2.22 Å [56] to 2.26 Å [62]. An estimate for the isolated anion of 2.283 Å has been made from an analysis of vibrational structure [63].

We find that the D_{2d} molecule is lower in energy than the D_{4h} system by 0.55 eV. We calculate that the observed distortion from T_d symmetry found in Cs_2CuCl_4 with an angle of 130° [62] is stable relative to the T_d geometry by 0.06 eV.

6.3. *Cobalt Chloride* $CoCl_4^{-2}$

The calculation was carried out on the $^4A_2$ ground state of $CoCl_4^{-2}$ using T_d symmetry and a Co–Cl bond length of 2.252 Å [64]. The results are compared in Table 10 with the restricted *ab initio* results of Hiller, Kenduck, Mabbs and Garner [64]. As in the $CuCl_4^{-2}$ results, we find that the unpaired t_2 MO's are not the HOMO's and that they lie at much lower energy: we surmise that the Coulomb repulsion energy is sufficiently large as to maintain these "holes" below doubly occupied ligand MO's. Figure 4 shows that the position of these metal $10t_2$ MO's causes the $9t_2\alpha$ MO's to be pushed up relative to the β MO's, and the $7t_2\alpha$ MO's to be pushed down. The end result of this is that the $9t_2$ average eigenvalue lies above the $3e$ and $2t_1$ average eigenvalues. We also calculate somewhat less $3d$ character in the $10t_2$ MO's and correspondingly more $4p$ character.

By again using a relaxation value of about 0.4 a.u. (or 0.44 a.u. as suggested in Table 10 comparing the α eigenvalue with the average eigenvalue) for the removal of a $3d$ electron and assuming the relaxation for the removal of an electron from a ligand orbital is small, the more classical ordering of the metal, ligand IP's is restored.

Comparison of the Mulliken population analysis shows that very good agreement is obtained for the atomic charges, but that for the Co atom the $3d$ and $4p$ balance

Table 10. $CoCl_4^{-2}$ results (a.u.)

	Ab initio [99] (restricted) ε_i	This work, INDO/1 ε_i α	β	average
$10t_2(3d)$[a]	0.1019(96)	−0.420(65)	[+0.538][b](68)	+0.060(67)
$2t_1$	−0.0862	−0.064	−0.062	−0.063
$3e$	−0.0984	−0.068	−0.064	−0.066
$9t_2$	−0.1123	−0.040	−0.068	−0.054
$8t_2$	−0.1409	−0.106	−0.109	−0.108
$8a_1$	−0.1809	−0.118	−0.111	−0.115
$2e(3d)$[a]	−0.3505(97)	−0.419(98)	−0.351(98)	−0.385(98)
$7t_2$	−0.6837	−0.548	−0.508	−0.528
$7a_1$	−0.6959	−0.549	−0.544	−0.546
Atomic charges:				
Cl	[−0.84][c]	−0.606 [−0.832][c]		
Co	[+1.36][c]	+0.422 [+1.330][c]		
Metal orbital populations:				
$3d$	[6.97][c]	7.147 [7.138][c]		
$4s$	[0.29][c]	0.444 [0.201][c]		
$4p$	[0.51][c]	0.984 [0.333][c]		

[a] Percentage Co $3d$ character.
[b] $10t_2$ β MO is unoccupied.
[c] Mulliken population analysis.

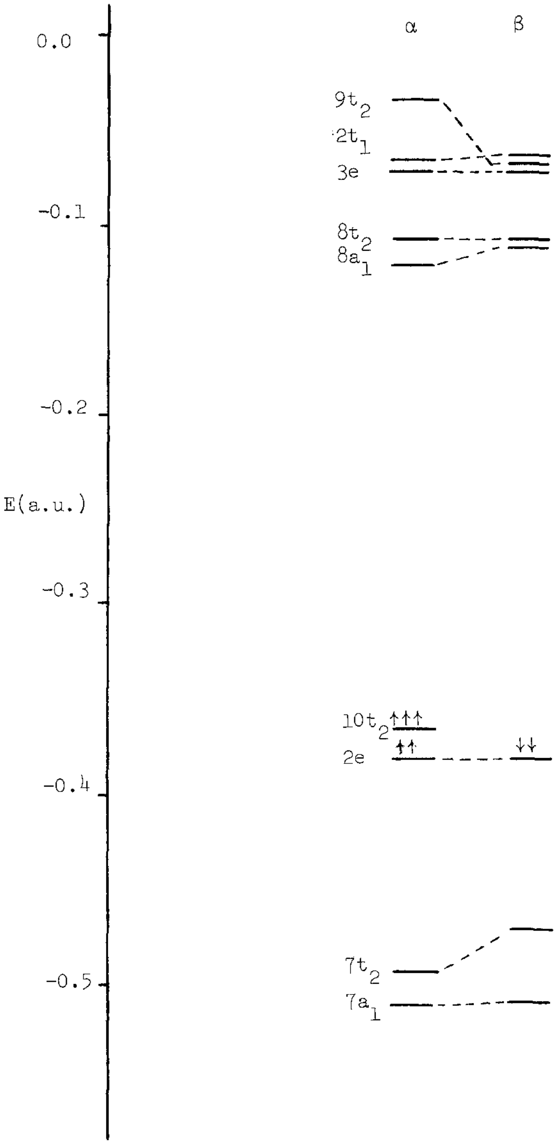

Fig. 4. Molecular orbital diagram for $CoCl_4^{-2}$. ↑ indicates the Co "3*d*" orbitals. All other orbitals of the diagram are occupied

is not in as good accord [59]. However, the *ab initio* calculation has a rather poor representation of the 4*s* and 4*p* AO's using only a single Gaussian function for each.

The eigenvalue of S^2 for this complex before spin annihilation is 3.750994, after, 3.750000. The annihilation has lowered the total energy by 0.0002 a.u.

Acknowledgements. This work has benefited greatly from interactions with Robert Kirchner, who aided with some of the programming, and with the Appendix. This work was supported in part through a research grant from the National Research Council of Canada.

Appendix

Below are listed all integrals that are included by the INDO model outlined in this work, and that are required to preserve rotational invariance. The abbreviation used is

$$\begin{array}{lllll} 0 = s & 1 = p_x & 2 = p_y & 3 = p_z & \\ 4 = d_{z^2} & 5 = d_{x^2-y^2} & 6 = d_{xy} & 7 = d_{xz} & 8 = d_{yz} \end{array}$$

There are other non-vanishing integrals under the INDO model, such as (04/00), etc., but these integrals are small, and their exclusion does not introduce rotational variance. They are all of Slater's "*R*" type [65].

An example of the importance of the mixed INDO terms that are kept can be seen in ferrocene [49]. The lowest lying singlet excitation is calculated as ${}^1E_1''(d_{z^2} \to d_\pi)$ at 22,000 cm^{-1}. The four states resulting from $d_{x^2-y^2}$, $d_{xy} \to d_{xz}(= d_\pi)$ are calculated nearly degenerate at 28,000 cm^{-1}, before configuration interaction (CI). These states then interact through (57/68), and after CI the resulting states, of ${}^1E_2''$ and ${}^1E_1''$ symmetry, are calculated split by 8000 cm^{-1} in reasonably good accord with the experimental value of 7000 cm^{-1}. Averaging over classes of integrals to avoid these mixed terms would give a very different assignment of the singlet absorption spectrum of ferrocene.

$$\begin{aligned}
(00/00) &= F_0(ss) \\
(01/01) &= (02/02) = (03/03) = G_1(sp) \\
(04/04) &= (05/05) = (06/06) = (07/07) = (08/08) = G_2(sd) \\
(11/00) &= (22/00) = (33/00) = F_0(sp) \\
(11/11) &= (22/22) = (33/33) = F_0(pp) + 4F_2(pp) \\
(12/12) &= (13/13) = (23/23) = 3F_2(pp) \\
(14/14) &= (24/24) = G_1(pd) + 18G_3(pd) \\
(14/15) &= (16/24) = (26/14) = -\sqrt{3}G_1(pd) - 3\sqrt{3}G_3(pd) \\
(15/15) &= (16/16) = (17/17) = (25/25) = (26/26) = (28/28) = (37/37) \\
&= (38/38) = 3G_1(pd) + 24G_3(pd) \\
(16/25) &= -3G_1(pd) + 21G_3(pd) \\
(17/34) &= (28/34) = 2\sqrt{3}G_1(pd) - 9\sqrt{3}G_3(pd) \\
(17/35) &= (18/18) = (18/27) = (18/36) = (27/27) = (27/36) = (35/35) \\
&= (36/36) = 15G_3(pd) \\
(22/11) &= (33/11) = (33/22) = F_0(pp) - 2F_2(pp) \\
(25/24) &= \sqrt{3}G_1(pd) + 3\sqrt{3}G_3(pd) \\
(26/15) &= 3G_1(pd) - 21G_3(pd) \\
(28/17) &= (37/15) = (37/26) = (38/16) = 3G_1(pd) - 6G_3(pd) \\
(28/35) &= -15G_3(pd) \\
(34/34) &= 4G_1(pd) + 27G_3(pd) \\
(37/14) &= (38/24) = -\sqrt{3}G_1(pd) + 12\sqrt{3}G_3(pd) \\
(38/25) &= -3G_1(pd) + 6G_3(pd) \\
(44/00) &= (55/00) = (66/00) = (88/00) = F_0(sd) \\
(44/11) &= (44/22) = F_0(pd) - 2F_2(pd)
\end{aligned}$$

$$(44/33) = F_0(pd) + 4F_2(pd)$$

$$\begin{aligned}(44/44) &= (55/55) = (66/66) = (77/77) = (88/88)\\ &= F_0(dd) + 4F_2(dd) + 36F_4(dd)\end{aligned}$$

$$(45/11) = (46/12) = -2\sqrt{3}F_2(pd)$$

$$(45/22) = 2\sqrt{3}F_2(pd)$$

$$(45/45) = (46/46) = 4F_2(dd) + 15F_4(dd)$$

$$(47/13) = (48/23) = \sqrt{3}F_2(pd)$$

$$(47/47) = (48/48) = F_2(dd) + 30F_4(dd)$$

$$\begin{aligned}(55/11) &= (55/22) = (66/11) = (66/22) = (77/11) = (77/33) = (88/22)\\ &= (88/33) = F_0(pd) + 2F_2(pd)\end{aligned}$$

$$(55/33) = (66/33) = (77/22) = (88/11) = F_0(pd) - 4F_2(pd)$$

$$(55/44) = (66/44) = F_0(dd) - 4F_2(dd) + 6F_4(dd)$$

$$(56/56) = 35F_4(dd)$$

$$(57/13) = (67/23) = (68/13) = (78/12) = 3F_2(pd)$$

$$(57/47) = (67/48) = (68/47) = \sqrt{3}F_2(dd) - 5\sqrt{3}F_4(dd)$$

$$(57/57) = (58/58) = (67/67) = (68/68) = (78/78) = 3F_2(dd) + 20F_4(dd)$$

$$(58/23) = -3F_2(pd)$$

$$(58/48) = -\sqrt{3}F_2(dd) + 5\sqrt{3}F_4(dd)$$

$$(58/67) = -3F_2(dd) + 15F_4(dd)$$

$$(66/55) = F_0(dd) + 4F_2(dd) - 34F_4(dd)$$

$$(68/57) = 3F_2(dd) - 15F_4(dd)$$

$$(77/44) = (88/44) = F_0(dd) + 2F_2(dd) - 24F_4(dd)$$

$$(77/45) = (78/46) = -2\sqrt{3}F_2(dd) + 10\sqrt{3}F_4(dd)$$

$$\begin{aligned}(77/55) &= (77/66) = (88/55) = (88/66) = (88/77)\\ &= F_0(dd) - 2F_2(dd) - 4F_4(dd)\end{aligned}$$

$$(88/45) = 2\sqrt{3}F_2(dd) - 10\sqrt{3}F_4(dd)$$

In the above,

$$\begin{aligned}F_0 &= F^0\\ G_1(sp) &= G^1(sp)/3\\ G_2(sd) &= G^2(sd)/5\\ G_3(pd) &= G^3(pd)/245\\ G_1(pd) &= G^1(pd)/15\\ F_2(pp) &= F^2(pp)/25\\ F_2(pd) &= F^2(pd)/35\\ F_2(dd) &= F^2(dd)/49\\ F_4(dd) &= F^4(dd)/441\end{aligned}$$

and the superscripted integrals are as defined in Ref. [65].

References

1. See, for example, Cotton, F. A.: Chemical applications of group theory, Chapt. 9. New York: Wiley-Interscience 1971; Ballhausen, C. J.: Introduction to ligand field theory. New York: McGraw-Hill 1962
2. Zerner, M. C., Gouterman, M. P.: Theoret. Chim. Acta (Berl.) **4**, 44 (1966)

3. Lohr Jr., L. L., Lipscomb, W. N.: J. Chem. Phys. **38**, 1607 (1963); Hoffmann, R.: J. Chem. Phys. **39**, 1397 (1963)
4. Pople, J. A., Beveridge, D. L., Dobosh, P. A.: J. Chem. Phys. **47**, 2026 (1967)
5. Pople, J. A., Santry, D. P., Segal, G. A.: J. Chem. Phys. **43**, S129 (1965); Pople, J. A., Segal, G. A.: J. Chem. Phys. **43**, S136 (1965); **44**, 3289 (1966)
6. Hall, M. B., Fenske, R. F.: Inorg. Chem. **11**, 768 (1972)
7. Zerner, M. C., Gouterman, M. P., Kobayashi, H.: Theoret. Chim. Acta (Berl.) **6**, 363 (1966)
8. Roothaan, C. C. J.: Rev. Mod. Phys. **23**, 69 (1951)
9. Pople, J. A., Nesbet, R. K.: J. Chem. Phys. **22**, 571 (1954)
10. Roothaan, C. C. J.: Rev. Mod. Phys. **32**, 179 (1960)
11. Hall, G. G.: Proc. Roy. Soc. (London) **A205**, 541 (1951)
12. Slater, J. C.: Quantum theory of atomic structure, Vol. I. New York: McGraw-Hill 1960
13. Clack, D. W.: Mol. Phys. **27**, 1513 (1974); Clack, D. W., Hush, N. S., Yandle, J. R.: J. Chem. Phys. **57**, 3503 (1972)
14. van der Lugt, W. T. A. M.: Intern. J. Quantum Chem. **6**, 859 (1972)
15. Figeys, H. P., Geerling, P., van Alsevoy, C.: Intern. J. Quantum Chem. **11**, 705 (1977)
16. Zerner, M. C., Parr, R. G.: J. Chem. Phys. **69**, 3858 (1978)
17. Zerner, M. C., in: Computational methods for large molecules and localized states in solids, Herman, F., McLean, A. D., Nesbet, R. K., eds. New York: Plenum Press 1972
18. Ridley, J. E., Zerner, M. C.: Theoret. Chim. Acta (Berl.) **32**, 111 (1973)
19. DelBene, J., Jaffé, H. H.: J. Chem. Phys. **48**, 1807 (1968); **48**, 4050 (1968)
20. Ridley, J. E., Zerner, M. C.: Theoret. Chim. Acta (Berl.) **42**, 223 (1976)
21. Bingham, R. C., Dewar, M. J. S., Lo, D. H.: J. Am. Chem. Soc. **97**, 1285, 1294, 1302, 1307 (1975); Dewar, M. J. S., Lo, D. H., Ramsden, C. A.: J. Am. Chem. Soc. **97**, 1311 (1975)
22. Dewar, M. J. S., Thiel, W.: J. Am. Chem. Soc. **99**, 4899, 4907, 5231 (1977); Dewar, M. J. S., Rzepa, H. S.: J. Am. Chem. Soc. **100**, 58 (1978)
23. Slater, J. C.: Phys. Rev. **36**, 57 (1930)
24. Clementi, E., Raimondi, D. L.: J. Chem. Phys. **38**, 2686 (1963)
25. Watson, R. E.: Phys. Rev. **119**, 1934 (1960)
26. Richardson, J. W., Nieuwpoort, W. C., Powell, R. R., Edgell, W. F.: J. Chem. Phys. **36**, 1057 (1962)
27. Clementi, E.: J. Chem. Phys. **41**, 303 (1964)
28. Richardson, J. W., Powell, R. R., Nieuwpoort, W. C.: J. Chem. Phys. **38**, 796 (1963)
29. Zerner, M. C.: Ph.D. Thesis, Harvard University, Cambridge, Mass. (1966)
30. Bacon, A. D.: M.Sc. Thesis, University of Guelph, Guelph, Ontario, Canada (1976)
31. Serafini, A., Savariault, J. M., Cassoux, P., Labarre, J. F.: Theoret. Chim. Acta (Berl.) **36**, 241 (1975)
32. Serafini, A., Pélissier, M., Savariault, J. M., Cassoux, P., Labarre, J. F.: Theoret. Chim. Acta (Berl.) **39**, 229 (1975)
33. Burns, G.: J. Chem. Phys. **42**, 1521 (1964)
34. Zerner, M. C.: Mol. Phys. **23**, 963 (1972)
35. Karlsson, G., Zerner, M. C.: Intern. J. Quantum Chem. **7**, 35 (1973)
36. Steubing, E. W., Weare, J. H., Parr, R. G.: Intern. J. Quantum Chem. **11**, 81 (1977)
37. Linderberg, J., Seamans, L.: Intern. J. Quantum Chem. **8**, 925 (1974)
38. Mulliken, R. S.: J. Chim. Phys. **46**, 497 (1949); **46**, 675 (1949)
39. Moore, C. E.: National Bureau of Standards Circular 467. Washington, D.C.: U.S. Dept. of Commerce 1949
40. Hinze, J., Jaffé, H. H.: J. Chem. Phys. **38**, 1834 (1963)
41. Anno, T., Teruya, H.: J. Chem. Phys. **52**, 2840 (1967)
42. Zerner, M. C.: unpublished results
43. Santry, D. P., Segal, G. A.: J. Chem. Phys. **47**, 158 (1967)
44. Benson, H. G., Hudson, A.: Theoret. Chim. Acta (Berl.) **23**, 259 (1971)
45. Coffey, P.: Intern. J. Quantum Chem. **8**, 263 (1974)
46. Löwdin, P. O.: Advan. Chem. Phys. **2**, 207 (1959)
47. Amos, T., Snyder, L. C.: J. Chem. Phys. **41**, 1773 (1964)

48. Amos, A. T., Hall, G. G.: Proc. Roy. Soc. (London) **A263**, 483 (1961)
49. Kirchner, R., Loew, G., Zerner, M. C.: to be published
50. Corrêa de Mello, P., Hehenberger, M., Zerner, M. C.: to be published
51. Richards, R. R., Gregory, N. W.: J. Phys. Chem. **69**, 239 (1965)
52. Noodleman, L.: J. Chem. Phys. **64**, 2343 (1976)
53. Slater, J. C.: Advan. Quantum Chem. **6**, 1 (1972)
54. Demuynck, J. A., Veillard, A., Wahlgren, U.: J. Am. Chem. Soc. **95**, 5563 (1973)
55. Willett, R. D.: J. Chem. Phys. **41**, 2243 (1964)
56. Helmholz, L., Kuch, R. F.: J. Am. Chem. Soc. **74**, 1176 (1952)
57. Demuynck, J., Veillard, A.: Chem. Phys. Letters **6**, 204 (1970)
58. Ros, P., Schmit, G. C. A.: Theoret. Chim. Acta (Berl.) **4**, 1 (1966)
59. Löwdin, P. O.: J. Chem. Phys. **18**, 365 (1950)
60. Figgis, B. N.: Introduction to ligand fields, p. 312. New York: Interscience 1966
61. Harlow, R. L., Wells III, W. J., Watt, G. W., Simonsen, S. H.: Inorg. Chem. **13**, 2106 (1974)
62. Harlow, R. L., Wells III, W. J., Watt, G. W., Simonsen, S. H.: Inorg. Chem. **14**, 1768 (1975)
63. McGinnety, J. A.: J. Am. Chem. Soc. **94**, 8406 (1972)
64. Hillier, I. H., Kenduck, J., Mabbs, F. E., Garner, C. D.: J. Am. Chem. Soc. **98**, 395 (1976)
65. Ref. [12], Chapt. 13

Received August 29, 1978/November 8, 1978